AMERICAN SOCIETY FOR MICROBIOLOGY | mBio

Check for updates

| Mycology | Research Article

Broad susceptibility of *Candida auris* strains to 8-hydroxyquinolines and mechanisms of resistance

Matthew B. Lohse,[1] Matthew T. Laurie,[2] Sophia Levan,[3] Naomi Ziv,[1] Craig L. Ennis,[4,5] Clarissa J. Nobile,[4,6] Joseph DeRisi,[2,7] Alexander D. Johnson[1]

AUTHOR AFFILIATIONS See affiliation list on p. 19.

ABSTRACT The fungal pathogen *Candida auris* represents a severe threat to hospitalized patients. Its resistance to multiple classes of antifungal drugs and ability to spread and resist decontamination in healthcare settings make it especially dangerous. We screened 1,990 clinically approved and late-stage investigational compounds for the potential to be repurposed as antifungal drugs targeting *C. auris* and narrowed our focus to five Food and Drug Administration (FDA)-approved compounds with inhibitory concentrations under 10 µM for *C. auris* and significantly lower toxicity to three human cell lines. These compounds, some of which had been previously identified in independent screens, include three dihalogenated 8-hydroxyquinolines: broxyquinoline, chloroxine, and clioquinol. A subsequent structure-activity study of 32 quinoline derivatives found that 8-hydroxyquinolines, especially those dihalogenated at the C5 and C7 positions, were the most effective inhibitors of *C. auris*. To pursue these compounds further, we exposed *C. auris* to clioquinol in an extended experimental evolution study and found that *C. auris* developed only twofold to fivefold resistance to the compound. DNA sequencing of resistant strains and subsequent verification by directed mutation in naive strains revealed that resistance was due to mutations in the transcriptional regulator *CAP1* (causing upregulation of the drug transporter *MDR1*) and in the drug transporter *CDR1*. These mutations had only modest effects on resistance to traditional antifungal agents, and the *CDR1* mutation rendered *C. auris* more susceptible to posaconazole. This observation raises the possibility that a combination treatment involving an 8-hydroxyquinoline and posaconazole might prevent *C. auris* from developing resistance to this established antifungal agent.

IMPORTANCE The rapidly emerging fungal pathogen *Candida auris* represents a growing threat to hospitalized patients, in part due to frequent resistance to multiple classes of antifungal drugs. We identify a class of compounds, the dihalogenated 8-hydroxyquinolines, with broad fungistatic ability against a diverse collection of 13 strains of *C. auris*. Although this compound has been identified in previous screens, we extended the analysis by showing that *C. auris* developed only modest twofold to fivefold increases in resistance to this class of compounds despite long-term exposure; a noticeable difference from the 30- to 500-fold increases in resistance reported for similar studies with commonly used antifungal drugs. We also identify the mutations underlying the resistance. These results suggest that the dihalogenated 8-hydroxyquinolines are working inside the fungal cell and should be developed further to combat *C. auris* and other fungal pathogens. Lohse and colleagues characterize a class of compounds that inhibit the fungal pathogen *C. auris*. Unlike many other antifungal drugs, *C. auris* does not readily develop resistance to this class of compounds.

Editor Deborah A. Hogan, Geisel School of Medicine at Dartmouth, Hanover, New Hampshire, USA

Address correspondence to Joseph DeRisi, joseph.derisi@ucsf.edu, or Alexander D. Johnson, ajohnson@cgl.ucsf.edu.

Matthew B. Lohse and Matthew T. Laurie contributed equally to this article. Author order was determined based on role in coordinating edits from other authors and submitting the manuscript.

Alexander D. Johnson and Clarissa J. Nobile are cofounders of BioSynesis, Inc., a company developing diagnostics and therapeutics for biofilm infections. Clarissa J. Nobile is acting CEO of BioSynesis, Inc. and Matthew B. Lohse is a consultant for BioSynesis, Inc. No funding for this research was provided by BioSynesis, Inc. and/or by any grants to BioSynesis, Inc. Neither BioSynesis, Inc. nor agencies funding BioSynesis, Inc. played any role in the study design, data collection and analysis, decision to publish, or preparation of the manuscript. Dr. DeRisi is a paid scientific consultant for Allen & Co., the Public Health Company, Inc., and a founder and scientific advisor for Delve Bio, Inc.. No funding for this research was provided by any of these entities, nor did they play any role in the study design, data collection and analysis, decision to publish, or preparation of the manuscript.

See the funding table on p. 19.

Received 7 June 2023
Accepted 13 June 2023
Published 26 July 2023

KEYWORDS *Candida auris*, antifungal resistance, dihalogenated 8-hydroxyquinolines, broxyquinoline, chloroxine, clioquinol, Cap1, Cdr1, Mdr1, drug repurposing screen, experimental evolution, structure-activity relationship

Candida auris is a rapidly emerging multidrug resistant pathogen responsible for invasive fungal infections in hospitalized patients. Similar to other *Candida* species, *C. auris* predominately induces candidemia in the immunocompromised and those subjected to prolonged hospitalization in intensive care unit wards or long-term care facilities. In untreated patients, invasive candidemia has a mortality rate of approximately 60%, which only improves to approximately 40% with antifungal therapy (1, 2). The threat of *C. auris* is compounded by persistent colonization in previously exposed patients and pervasive spread through hospital wards despite multiple rounds of decontamination (3, 4). Furthermore, *C. auris* can spread through long-term care and skilled nursing facilities with older and ventilator-dependent patients being especially at risk for infection; several *C. auris* outbreaks associated with COVID-19 treatment units have been reported (5–9). This pervasive colonization, in combination with frequent resistance to one, two, or even all three major classes of antifungals, makes *C. auris* a growing threat to our most vulnerable patients (10). For these reasons, the World Health Organization's recently released fungal priority pathogens' list includes *C. auris* as one of four fungal pathogens in the critical (as opposed to high or medium) priority group (11).

C. auris represents a relatively new threat to hospitalized patients. It was first reported in Japan in 2009 (12) and was subsequently found to have five clades (I–V) that localize to distinct geographic locations (13, 14). The five clades, which are geographically represented by South Asia (I), East Asia (II), Africa (III), South America (IV), and Iran (V), have different frequencies of antifungal resistance and two distinct mating types (13–16). Clades I, III, IV, and V have been linked to outbreaks of invasive infections while clade II is more commonly associated with ear infections (17, 18). While specific clades typically predominate in different parts of the world, the US, Canada, UK, and Kenya have identified infections associated with a range of isolates from multiple clades (16, 19–21). Nearly all *C. auris* isolates are highly resistant to fluconazole; more than half are resistant to voriconazole; a third are resistant to amphotericin B; and some isolates are resistant to all three major classes of antifungal drugs including the echinocandins caspofungin and micafungin (16, 22–26). Given the high mortality, limited treatment options, and growing threat to vulnerable patient populations, there is an urgent need to develop new antifungal agents to combat *C. auris*.

Several approaches have been taken to identify new antifungal agents effective against *C. auris* [for more detail on this topic and the current state of the antifungal drug development pipeline, see references (27–33)]. The most straightforward approach has focused on the evaluation of the effectiveness of the newest members of common antifungal classes (e.g., the echinocandin rezafungin [CD101]) (34, 35). A closely related line of investigation has focused on testing the lead compound(s) from new classes of potential antifungal agents in development and/or in the clinical testing pipeline [e.g., the fungal inositol acylase inhibitor fosmanogepix/APX001 (36–38) and the glucan synthesis inhibitor ibrexafungerp/SCY-078 as well as the second generation fungerp analog SCY-247 (39–43)]. A broader approach, and one less dependent on existing antifungal drug development pipelines, involves screening libraries of Food and Drug Administration (FDA)-approved compounds and/or drug like compounds to repurpose existing clinical compounds for use against *C. auris*. These types of screens have identified a number of promising compounds, including ebselen, miltefosine, and alexidine dihydrochloride. Three of these published screens were conducted with the same library (the Prestwick Chemical Library with 1,280 compounds), but the hits from these screens were not always concordant (49 different compounds were identified in these screens: 3 in all three, 18 in two, and 28 in only one) (44–49).

To identify potential drug repurposing candidates, we conducted a broad primary drug screen that examined the effect of 1,990 clinically approved or late-stage

investigational compounds on three *C. auris* strains from the clades most associated with invasive infections (I, III, and IV). From the 86 candidate compounds identified during this preliminary screen, we found five FDA-approved compounds with half-maximal inhibitory concentrations (IC_{50}) that were less than 10 µM for *C. auris* and at least an order of magnitude lower in toxicity to three human cell lines. For one of these compounds, the 8-hydroxyquinoline clioquinol, we identified mutations conferring resistance by growing two *C. auris* isolates for an extended period in the presence of the compound, followed by whole genome sequencing. To prove that the mutations we identified caused the resistance, we reconstructed the mutations in a naïve strain (using CRISPR-based approaches) and showed they conferred resistance.

RESULTS

The hydroxyquinolines namely broxyquinoline, chloroxine, and clioquinol inhibit *C. auris* growth at submicromolar concentrations

A primary screen of 1,990 compounds, consisting of clinically approved drugs, late-stage investigational compounds, and drug-like compounds, was performed using three strains of *C. auris* that were selected based on their range of resistance to the three main classes of antifungal agents and to represent the three clades most associated with invasive infections (Fig. 1A). Strain AR-387 (B8441/MLY1543) originated in Pakistan, belongs to clade I, and is susceptible to fluconazole, caspofungin, and amphotericin B. Strain AR-386 (B11245/MLY1542) originated in Venezuela, belongs to clade IV, is susceptible to both caspofungin and amphotericin B but resistant to fluconazole. Strain AR-384 (B11222/MLY1540) originated in South Africa, belongs to clade III, is susceptible to amphotericin B and resistant to both fluconazole and caspofungin.

These three strains were screened for growth inhibition at two concentrations (1 µM and 10 µM) of drugs from the Selleck Chem FDA-Approved Drug Library (#L1300, 1,591 compounds) and the Medicines for Malaria Venture Pandemic Response Box (399 compounds) (Fig. 1A). Compounds with a B-score [a non-control based method accounting for systematic errors including plate position effects (50, 51)] greater than 0.1 and greater than 50% inhibition (measured by optical density at 600 nm [OD_{600}]) were considered initial hits (Fig. 1B; File S1). The 86 initial hits include 10 established standard-of-care compounds for fungal infections, 44 compounds active against only two of the three *C. auris* strains tested, and 32 compounds active against all three (Fig. 1B; File S1). A secondary screen was performed to confirm the antifungal activity observed in the primary screen and to estimate the half maximal inhibitory concentrations (IC_{50}s) for these compounds (Fig. 1C). All 86 compounds were screened at eight concentrations ranging from 0.3 to 100 µM against the same three strains (AR-387, AR-386, and AR-384) (Fig. 2A; File S1). We then selected 11 compounds that had estimated IC_{50}s less than 10 µM in this secondary screen and did not belong to the three main known classes of antifungal drugs. Three additional compounds (sirolimus, everolimus, and temsirolimus) met these criteria, but were not selected for further investigation because of their known immunosuppressive activity.

An optimal drug candidate would have antifungal activity against a wide range of *C. auris* isolates at concentrations that are not toxic to human cells. To determine if any of the 11 selected compounds fulfilled these criteria, IC_{50}s were determined for 16 *Candida* strains, including 13 *C. auris* strains, covering all five clades, and one strain each of *Candida albicans*, *Candida glabrata*, and *Candida dubliniensis*. The IC_{50}s of these 11 compounds were also determined for three common human cell lines, HEK293 (kidney), HEPG2 (liver), and HFF1 (fibroblast) (Fig. 1C). Of the 11 compounds, five had IC_{50}s that were at least 10-fold less than their lowest IC_{50} for human cells, suggesting the possibility of a therapeutic window (Fig. 2B). These five compounds included three hydroxyquinolines, broxyquinoline, chloroxine, and clioquinol, and two anti-protozoals, miltefosine and triclabendazole (Fig. 2B). We observed a smaller range of IC_{50}s across the 13 *C. auris* strains for miltefosine (minimum IC_{50} 1.5 µM, maximum IC_{50} 4.9 µM, threefold range), broxyquinoline (minimum IC_{50} 0.16 µM, maximum IC_{50} 0.33 µM, twofold range),

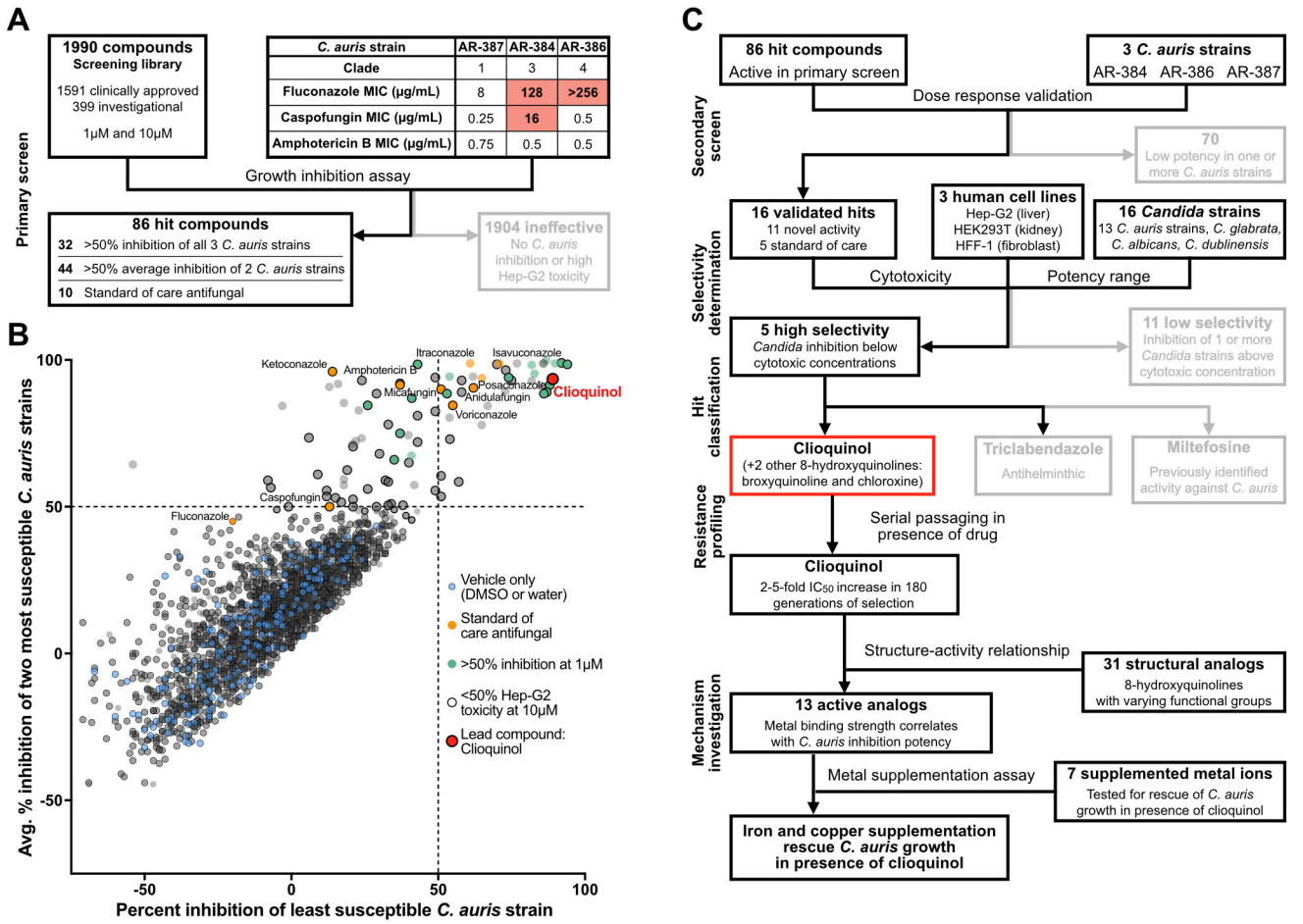

FIG 1 A screen of 1,990 clinically approved and investigational compounds for *in vitro* inhibition of *C. auris* identified 86 candidates for further evaluation. (A) Workflow for the primary screening of 1,990 clinically approved and investigational compounds for *in vitro* inhibition of three *C. auris* strains; compounds were screened at both 1 µM and 10 µM. (B) The percent inhibition relative to untreated controls (DMSO or water alone) for each compound at 10 µM. For each compound, the lowest percent inhibition achieved against any of the three screened *C. auris* strains is plotted on the *x*-axis and the average percent inhibition against the other two strains is plotted on the *y*-axis. Compounds in the upper left quadrant effectively inhibited two of the three *C. auris* strains and compounds in the upper right quadrant effectively inhibited all three strains. (C) The secondary screening pipeline for the 86 compounds identified in the initial screen for their ability to inhibit at least two of the three *C. auris* strains by at least 50%. Additional screening monitoring inhibition of additional *C. auris* strains, other *Candida* species, and lack of toxicity to human cells yielded five highly selective candidates (see Fig. 2). Figures 3 and 4 detail additional criteria depicted in the flow chart.

chloroxine (minimum IC_{50} 0.39 µM, maximum IC_{50} 0.94 µM, twofold range), and clioquinol (minimum IC_{50} 0.12 µM, maximum IC_{50} 0.58 µM, fivefold range) than many traditional antifungal agents, for example, caspofungin (minimum IC_{50} 0.15 µM, maximum IC_{50} 73 µM, 500-fold range) and posaconazole (minimum IC_{50} 0.01 µM, maximum IC_{50} 0.43 µM, 43-fold range) (Fig. 2B; File S1). In other words, the IC_{50}s for the compounds identified in the screen were more consistent across the different *C. auris* strains than were the IC_{50}s for many of the existing antifungals. These results are broadly consistent with previous repurposing screens, which have reported effectiveness by miltefosine (46), several different hydroxyquinolines including chloroxine and clioquinol (45–47, 49, 52–54), as well as pentamidine (one of the six compounds that performed poorly in our human cell toxicity tests) (44, 46). Although 12 of the 13 *C. auris* strains were taken from the Centers for Disease Control and Prevention's Antibiotic Resistance Isolate Bank *Candida auris* panel, this panel encompasses a wide range of susceptibilities to different antifungal agents and, as such, we believe these results are broadly applicable to *C. auris*.

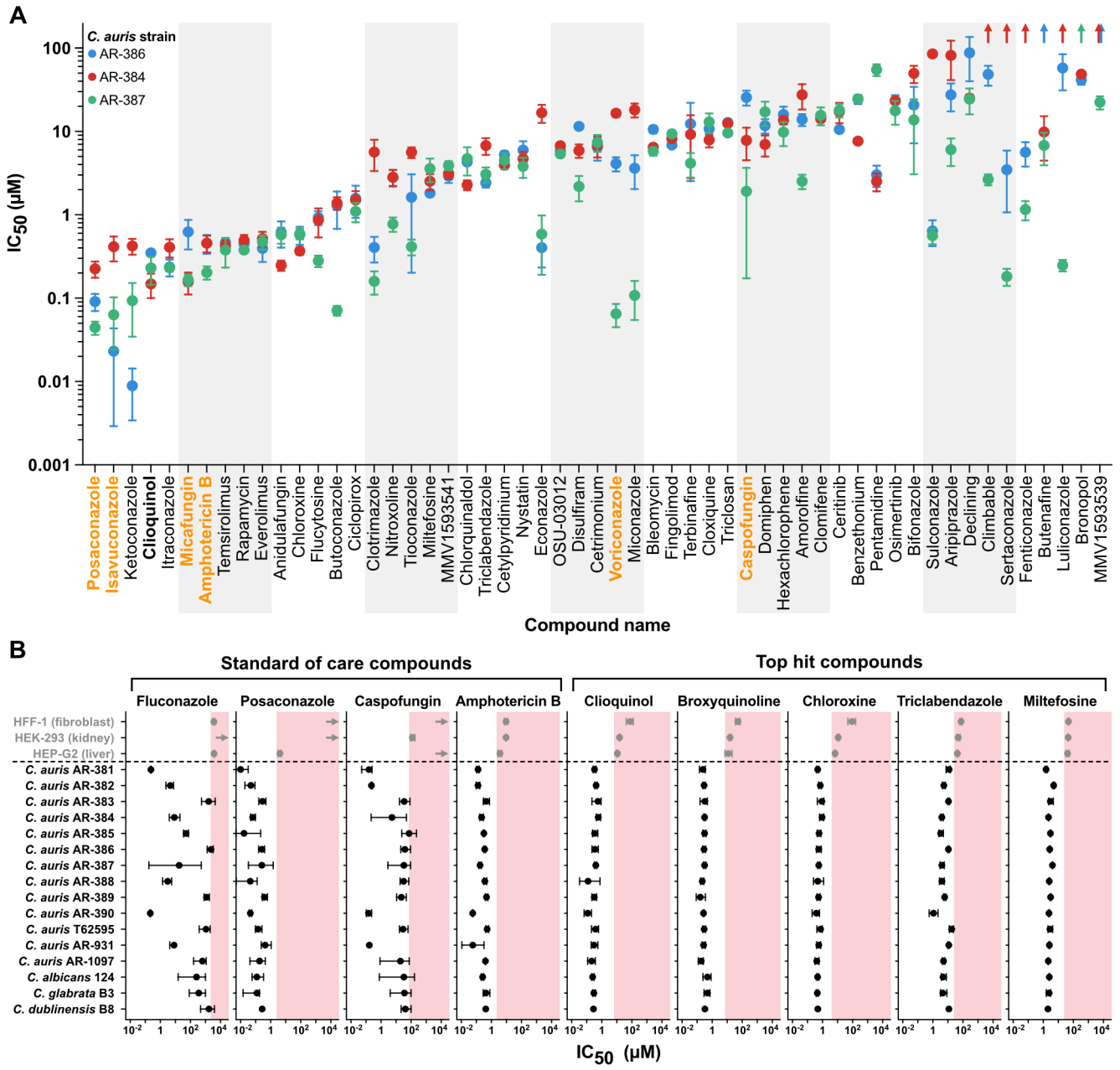

FIG 2 Secondary screening and selectivity measurement identified five promising compounds, including three hydroxyquinolines. (A) In the secondary screen, the results with 31 of the 86 hits identified in the primary screen did not repeat and were eliminated from further consideration. IC_{50} values against three *C. auris* strains for the remaining 55 compounds were calculated from 8-point dose-response curves. Points represent the mean of three biological replicates, error bars represent the standard error of the mean, and upwards arrows indicate IC_{50} values greater than the highest concentration tested, 100 μM. Representative standard-of-care compounds used to treat fungal infections are indicated in orange. (B) IC_{50} values for four standard-of-care drugs and five finalists from the screen against 13 *C. auris* strains, strains from three additional *Candida* species, and three human cell lines. Pink shaded regions mark concentrations above the lowest observed IC_{50} for that compound against a human cell line. Values represent the IC_{50} calculated from three biological replicates, error bars represent the 95% confidence interval, and right-pointing arrows indicate IC_{50} values greater than 1,000 μM.

C. auris develops only moderate resistance to clioquinol despite extended exposure

C. auris has repeatedly demonstrated a propensity for rapid acquisition of resistance when exposed to antifungal drugs. Indeed, experimental evolution studies have produced 30-fold to more than 500-fold increases in resistance to fluconazole or

caspofungin in as few as two or three 24- or 48-h passages (55–57). To evaluate the ability of *C. auris* to develop resistance to clioquinol, and to assess the resulting determinants of resistance, two independent cultures of *C. auris* AR-384 (discussed above) and one culture of AR-390, another clade I strain with greater resistance to fluconazole and amphotericin B than AR-387, were serially passaged 30 times (roughly 150–200 generations) in the presence of increasing concentrations of clioquinol, ranging from 0.4 to 0.75 µM at the start to 2.8-4.4 µM at the end (Fig. 1C). By the end of the drug selection, the clioquinol IC_{50} increased 2.4- and 5.2-fold relative to parental strains (from 0.75 µM to 1.80 µM and from 0.29 µM to 1.48 µM) in the AR-384 and AR-390 backgrounds, respectively (Fig. 3A and B). The IC_{50} increases occurred over multiple steps, showed some variation in the rate of resistance evolution, and leveled off around passage 16 for each culture (Fig. 3A). Notably, the degree of resistance arising from more than 2 months of exposure to clioquinol was less than that has been observed for fluconazole or caspofungin over shorter time frames. Furthermore, the clioquinol-evolved strains remained susceptible to clioquinol concentrations at least fivefold below the minimal toxic concentrations observed for human cells.

Mutations in the genes *CAP1* and CDR1 arose during extended clioquinol exposure and are the cause of resistance

The resistance of the evolved strains persisted when these strains were regrown for several days in the absence of clioquinol, indicating that resistance was linked to one or more genome mutations rather than a reversible, physiological response to clioquinol. To test this hypothesis and identify the determinant(s) of clioquinol resistance, we performed whole genome sequencing on two single colony isolates from the endpoint of the resistance experiment for each of the three cultures as well as from populations harvested from selected intermediate points. We observed premature termination mutations in the C-terminal end of the transcriptional regulator *CAP1* (B9J08_005344/CJI97_005427) by the eighth passage in all three cultures (16 days growth or approximately 35 to 40 generations) (Fig. 3A). Each mutation was distinct (E398* in AR-390; either E441* or an 8 bp deletion resulting in T387* in AR-384) and was in 76% to 98% of the population sample reads at passage eight. The same *CAP1* mutations were in 96% to 98% of population sample reads and in all six single cell samples at the endpoint of the experiment. *CAP1* mutations were not observed in the dimethyl sulfoxide (DMSO) treated control cultures that were grown and sequenced in parallel. Based on additional experiments described below, we believe these truncation mutations produce hyperactive Cap1 proteins.

Sometime after the eighth passage (by passage 12 in AR-390 and between passages 8 and 31 in AR-384), additional mutations arose in the ATP-binding cassette drug transporter *CDR1* (B9J08_000164/CJI97_000167). The mutations in this gene were different in the three cultures, and likely result in loss of function of the gene (see below; E722* in AR-390; K909N or Q415* in one AR-384 culture; and Q548* or an 8 bp deletion whose resulting frame shift affected 34 different amino acids at aa343–376 before a premature stop codon at aa377 in the other AR-384 culture) (Fig. 3A). These *CDR1* mutations were not as prevalent in the populations as the *CAP1* mutations, comprising between 25% and 97% of reads in population samples and were observed in only four of the six single-cell endpoint samples. No *CDR1* mutations were observed in the DMSO-treated control cultures. We note that the apparent selective pressure to inactivate the *CDR1* drug pump suggests that hydroxyquinolines function against *C. auris*, at least in part, at the cell surface or inside the cell rather than by chelating soluble iron, copper, or zinc in the media, consistent with a previous report that hydroxyquinolines sequester metals in *Saccharomyces cerevisiae's* plasma membrane (58). It may seem paradoxical that inactivating a drug pump results in increased resistance—rather than susceptibility—to clioquinol; however, in addition to exporting drugs, *CDR1* has been implicated in the translocation of phosphoglycerides from the internal to the external plasma membrane (59, 60). In principle, the hydroxyquinolines could be affecting another function of Cdr1

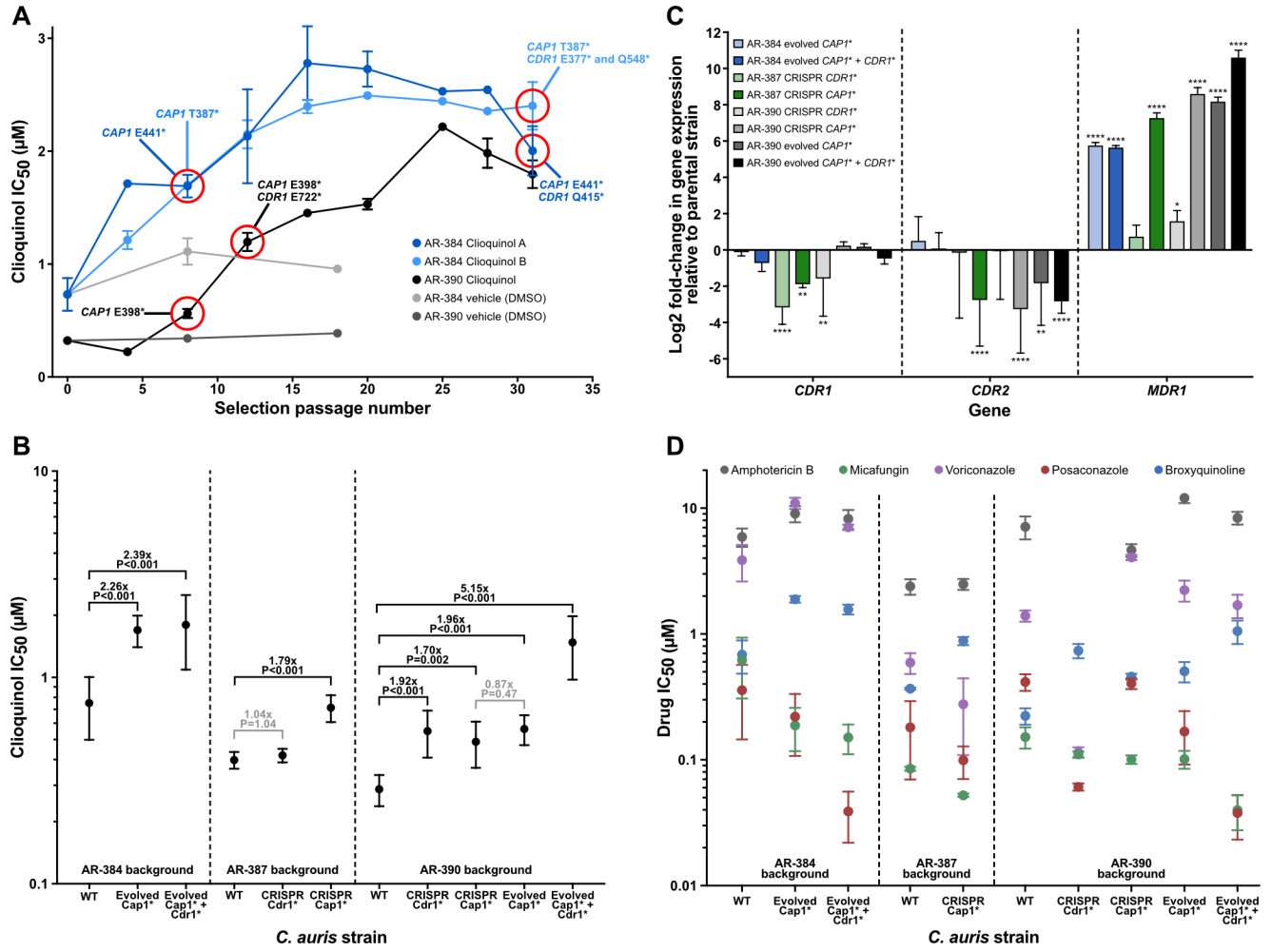

FIG 3 *C. auris* developed 2- to 5-fold resistance to clioquinol in an extended evolution experiment due to mutations in the transcriptional regulator *CAP1* and the *CDR1* drug pump. (A) Clioquinol IC_{50} against *C. auris* isolates that were selected in the presence of clioquinol. Parallel cultures were grown with serial passaging of strains AR-384 (blue, two independent cultures) and AR-390 (black, one culture) in the presence of clioquinol or vehicle control (DMSO; grey). Whole genome sequencing was performed for a subset of *C. auris* passage populations or single cells isolated from the cultures and selected mutations identified are indicated. Error bars represent the standard error of the mean. (B) Comparison of clioquinol's IC_{50} against parent, evolved, and CRISPR/Cas9 engineered *C. auris* mutant strains from three different backgrounds. The fold-changes in IC_{50} between relevant related strains are shown; the statistical significance of observed differences as determined with unpaired t-tests (two-tailed, equal variance) is indicated. Error bars represent the standard deviation. (C) Changes in expression of the *CDR1*, *CDR2*, and *MDR1* drug pump genes in evolved and CRISPR/Cas9 engineered *C. auris CAP1* and *CDR1* mutant strains from three different backgrounds in the absence of clioquinol. Gene expression changes are shown as the Log2 fold-change relative to the parental (WT) strain for that background. Statistical significance was determined with unpaired t-tests (two-tailed, equal variance, $*P < 0.05$; $**P < 0.01$; $***P < 0.001$; $****P < 0.0001$). Error bars represent the standard deviation. (D) Comparison of IC_{50} values for five other drugs against parent, evolved, and CRISPR-Cas9 engineered mutant *C. auris* strains. Values represent the mean of three independent experiments; error bars represent the standard error of the mean.

instead of, or in addition to, exporting drugs from the cell. It is also possible that Cdr1 functions to import hydroxyquinolines into the cell.

To determine whether the *CAP1* or *CDR1* mutations were indeed causal for increased clioquinol resistance, the *CAP1* E398* and the *CDR1* E722* mutations were introduced by CRISPR-Cas9 gene editing into the parental strains AR-390 and AR-387. The *CAP1* E398* mutation caused an increase in resistance of 1.7- to 1.8-fold to clioquinol in both strains (Fig. 3B), similar to that observed for the evolved *CAP1** strains, indicating that the *CAP1* mutation is the cause of resistance in the evolved strains. Introducing the *CDR1* E722* mutation did not significantly affect clioquinol resistance in AR-387 (nor did deletion of *CDR1*) but it did increase resistance 1.9-fold in AR-390 (Fig. 3B). Thus, the *CAP1* truncation (which results in a gain-of-function mutation, see below) can explain much of

the clioquinol resistance that arose during the experimental evolution; the subsequent *CDR1* mutation (which likely results in a loss-of-function) could account for the smaller resistance increases observed later in the experiment.

CAP1 truncation results in increased *MDR1* expression

Cap1 is a transcriptional regulator. In *C. albicans*, it promotes expression of the major facilitator superfamily drug transporter *MDR1,* and it has been reported that C-terminal truncations of *CAP1*, like those we isolated from our drug-resistance screen, cause a hyperactive phenotype which increases *MDR1* expression and thereby increases fluconazole resistance (61–64). To test whether this is also the case with our resistant *C. auris CAP1* mutants, we used quantitative reverse transcription-polymerase chain reaction (RT-qPCR) to examine the levels of *MDR1* expression along with two other drug transporters: *CDR1* and *CDR2*. We found that *MDR1* expression had increased more than 50-fold by passage 8 in the AR-384 background compared to the starting strain and remained at this level at the end of the experiment (Fig. 3C). In the AR-390 background, where baseline expression began roughly 30-fold lower than AR-384, *MDR1* expression increased nearly 300-fold compared to the starting strain by passage 8 and over 1,500-fold by the final selection passage, reaching a similar level to the evolved AR-384 strains (Fig. 3C). In contrast to *MDR1*, expression of *CDR1* and *CDR2* changed only minimally during the course of the selection experiment (1.7-fold down and 1.1-fold up in AR-384, 1.4-fold down and 7-fold down in AR-390, respectively) (Fig. 3C). We note that we profiled transcript levels in the cells in the absence of clioquinol; thus, the changes we observed are due to the mutations and are not dependent on the presence of the compound.

To verify these results, transcript levels were also assessed in the mutant stains constructed in the AR-387 and AR-390 strain backgrounds, again in the absence of clioquinol. Consistent with the results for the evolved strains, the replacement of the wild-type *CAP1* with the *CAP1* E398* mutation resulted in minimal expression change for *CDR1* and *CDR2*, but 150- and 390-fold increases in *MDR1* expression in the AR-387 and AR-390 strain backgrounds, respectively (Fig. 3C). The results of these experiments show that *MDR1* expression is significantly increased by truncation mutations in *CAP1* both in the evolved strains and the genetically modified strains.

The link between *MDR1* transcript levels and susceptibility to clioquinol is also supported by recent work on the transcriptional regulator Mrr1. Two independent studies reported that a hyperactive Mrr1 allele (N647T) found in several clade III *C. auris* isolates results in upregulation of *MDR1*; of particular interest is the observation that *MDR1* transcript levels are approximately 18-fold higher in the clade III strain AR-383 than the clade I strain AR-390 (65, 66). Consistent with increases of *MDR1* expression reducing clioquinol susceptibility, we note that AR-383 is less susceptible to clioquinol than AR-390 (IC_{50} of 0.56 µM versus 0.12 µM, File S1).

Extended clioquinol exposure has only modest effects on resistance to traditional antifungal agents

The *CAP1* truncation mutations that arose in response to clioquinol could plausibly produce resistance to the existing antifungal agents used to treat *C. auris* infections. Conversely, given the role of *CDR1* in azole resistance (48, 67–71), the *CDR1* mutations that arose in our drug-resistant cultures could increase susceptibility to existing antifungal agents. To test this hypothesis, the susceptibilities of the evolved strains to a second hydroxyquinoline, broxyquinoline, and to the traditional antifungal agents voriconazole, posaconazole, micafungin, and amphotericin B were determined. As expected, the modest clioquinol resistance was also observed for the structurally similar broxyquinoline (Fig. 3D). Clioquinol resistance had only a subtle, if any, effect on susceptibility to amphotericin B, modestly increased susceptibility to micafungin (fourfold), and modestly increased (less than threefold) resistance to the azole voriconazole (Fig. 3D). An unexpected property of the evolved strains containing the *CDR1*

loss-of-function mutation was its 10-fold greater susceptibility to the azole posaconazole (Fig. 3D). These findings indicate that, for *C. auris*, mutations resulting from long-term exposure to clioquinol will not necessarily result in increased resistance to commonly used antifungal agents. Indeed, these observations suggest that combining an 8-hydroxyquinoline with posaconazole might leave *C. auris* especially vulnerable to the latter.

A variety of dihalogenated hydroxyquinolines inhibit *C. auris*

As described above, three hydroxyquinolines with submicromolar antifungal activity against *C. auris* were identified in our screen. To evaluate the structure-activity relationship (SAR) of this class of compounds, the activities of 32 quinoline derivatives (29 compounds plus clioquinol, broxyquinoline, and chloroxine, the three identified in the screen) were tested against three strains of *C. auris* (AR-387, AR-384, and AR-386) (Fig. 1C). Seventeen of these compounds showed activity against all three *C. auris* strains tested. All active compounds except for one [1,10-phenanthroline monohydrate] were hydroxyquinolines, which have a hydroxide at C8 position (Fig. 4A; File S1). Five compounds, including clioquinol, broxyquinoline, and chloroxine, had an IC_{50} less than 1 µM; all five of these compounds were dihalogenated at the C5 and C7 positions, suggesting the importance of these modifications in antifungal activity. Compounds with single halogen or other chemical groups at either the 5- or 7-positions generally had an IC_{50} in the 2 to 20 µM range, only four of the 20 compounds with a hydroxide at C8 position lacked activity against *C. auris*. Eleven of the 12 compounds without an 8-position hydroxy group tested lacked activity against *C. auris* (Fig. 4A; File S1). We note that these trends are largely consistent with those previously reported for halogenated hydroxyquinoline activity against several fungal species, none of which were *Candida* (72–74).

Previous studies (including transcriptional profiling, enzyme activity assays, and cellular metal abundance quantification using inductively coupled plasma mass spectrometry) showed that *S. cerevisiae* cells treated with clioquinol behave as if they are starved for iron, copper, and zinc. These metals are sequestered in the plasma membrane and depleted in the cytosol of *S. cerevisiae* cells exposed to clioquinol (58, 75, 76). To investigate this effect with respect to *C. auris*, clioquinol treated cells were grown in the presence of excess iron, copper, or zinc (Fig. 1C). The addition of excess iron (either Fe^{2+} or Fe^{3+}) or, to a lesser extent, copper, to clioquinol-treated media mitigated the inhibitory effects of the drug and restored growth (Fig. 4B and C). Increasing concentrations of Cu^{2+}, Fe^{2+}, or Fe^{3+} strongly correlated with increased clioquinol IC_{50}, indicating that the increase in *C. auris* viability is concentration dependent (Fig. 4C). Increasing concentrations of Zn^{2+}, on the other hand, had no effect on clioquinol IC_{50} (Fig. 4C). Addition of excess iron or copper also restored growth in the presence of several other 8-hydroxyquinolines (Fig. 4B). These effects were independent of the order of addition: either introducing iron to *C. auris* cells that had been pretreated with clioquinol for 21 h or introducing metals to clioquinol-treated media prior to *C. auris* inoculation permitted growth (Fig. 4B; Fig. S1A).

We note that the reversal of the inhibitory effects of hydroxyquinolines by exogenously added metals could be due, at least in part, to simply lowering the free concentration of hydroxyquinolines in the media. In this regard, the concentration of metals needed to overcome the inhibitory effects is in the same range as the concentrations of hydroxyquinolines needed to inhibit *C. auris*. The exact mechanisms by which hydroxyquinolines inhibit *C. auris* growth remain to be determined. It is a plausible hypothesis that the inhibitory effects arise from metal sequestration within the cell, perhaps in the fungal plasmid membrane as observed in *S. cerevisiae* (58). This idea is consistent with our observations that drug pump expression plays a role in the mechanism of resistance.

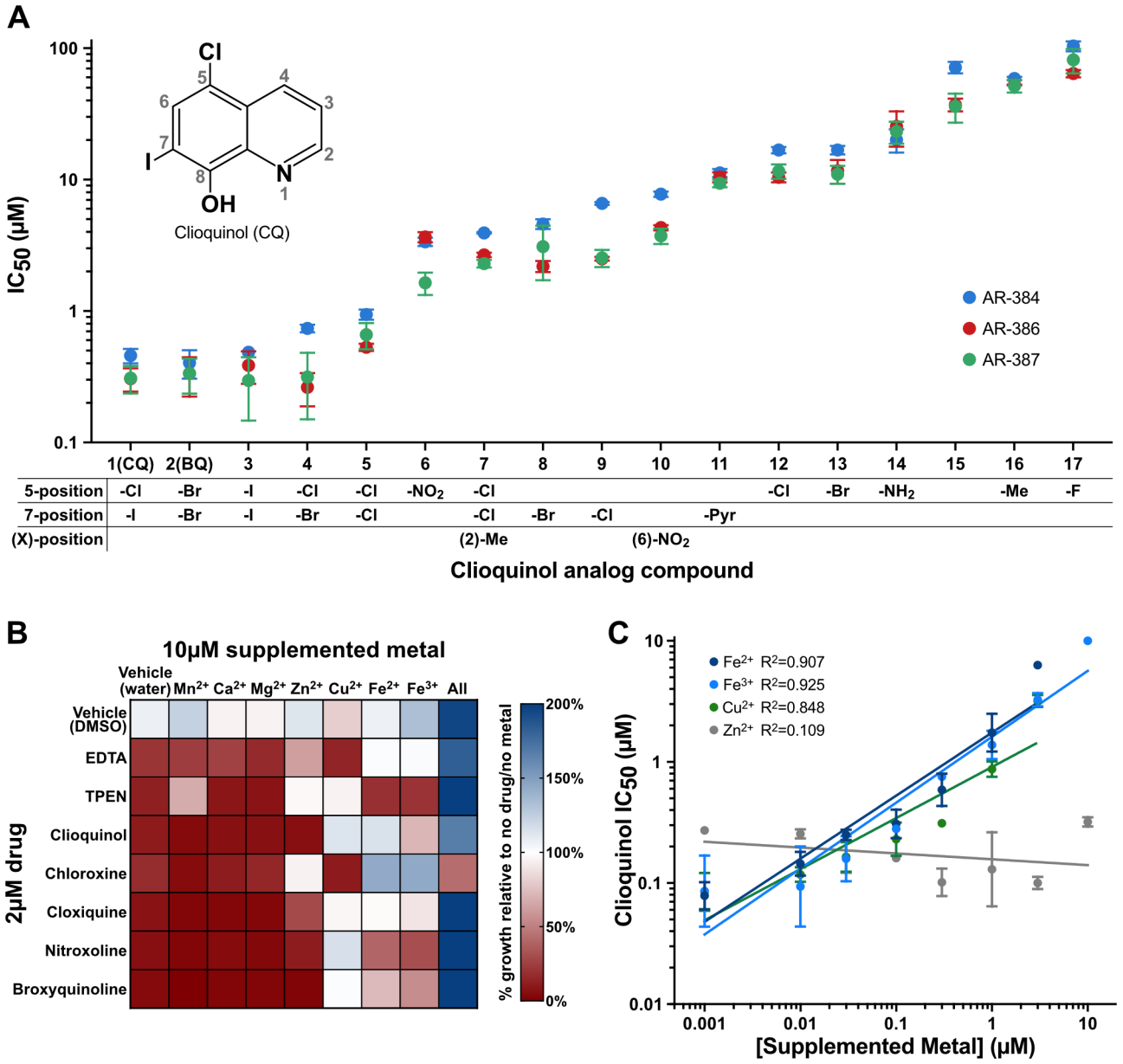

FIG 4 Out of the 32 SAR compounds (including clioquinol), dihalogenated 8-hydroxyquinolines were the most effective inhibitors of *C. auris*, and their activity is mitigated by excess iron or copper in the growth medium. (A) IC_{50} of clioquinol and 16 structural analogs against three *C. auris* strains. Clioquinol (upper left inset) is composed of a quinoline core with a 5-position chlorine, 7-position iodine, and 8-position hydroxy group, the functional groups at these and other positions are indicated for each of the structural analogs. A further 15 clioquinol analogs (not shown) were tested and lacked activity against *C. auris*. Error bars represent the standard error of the mean. (B) Heat map of *C. auris* growth (with and without 8-hydroxyquinoline compounds) in the presence of 10 μM metal ions. The effects of metal chelators EDTA and TPEN were also analyzed. The 8-hydroxyquinolines and the metal chelators inhibited growth (red on heat map) and addition of iron or copper mitigated these effects in at least some strains. (C) Relationship between supplemented metal concentration and clioquinol IC_{50}. The linear regression line is shown for each metal. The points represent the mean of three independent experiments; error bars represent the standard error of the mean.

Clioquinol is fungistatic to *C. auris*

Previous reports have reached different conclusions as to whether clioquinol is fungistatic or fungicidal against *Saccharomycotina* species such as *S. cerevisiae* or *C. albicans* (77, 78). We quantified, by plating assays, the viability of *C. auris* cells treated with clioquinol for 22 h and found that viability changed little relative to DMSO-treated

controls (Fig. S1B). As such, we conclude that clioquinol is fungistatic, rather than fungicidal, to *C. auris*, at least in the 22-h time frame examined.

DISCUSSION

C. auris represents a growing threat to hospitalized patients due to (1) the inherent resistance of many strains to one or more of the three major classes of antifungal drugs used in the clinic, (2) the propensity for susceptible *C. auris* strains to rapidly develop resistance to standard antifungal treatments, and (3) its ability to spread and resist decontamination in healthcare settings. We screened 1,990 compounds for the potential to be repurposed as antifungal agents targeting *C. auris*. Among the most promising hits from this screen were the dihalogenated hydroxyquinolines broxyquinoline, chloroxine, and clioquinol. A further structure-activity relationship study identified two additional, related compounds. Dihalogenated hydroxyquinolines have been identified in other small molecule screens for activity against *C. auris*, and we pursued this class of compounds further.

The five hydroxyquinolines mentioned above had IC_{50}s less than 1 µM and are especially interesting candidates for repurposing. First, the clinical isolates we tested (13 strains, including representatives of all five known clades) exhibited similar susceptibilities to 8-hydroxyquinolines suggesting that, unlike traditional antifungal drugs, there is little inherent resistance to the hydroxyquinolines. Second, although the dihalogenated hydroxyquinolines were the most efficient hydroxyquinolines in our SAR screen, a wide range of chemical space in this family remains to be explored (e.g., different side groups at C2 and different active groups replacing the halogen at C5 or C7). Further underscoring the potential of this chemical space, the antimalarial compound mefloquine (a quinolinemethanol derivative with a core structure similar to the 8-hydroxyquinolines) also has broad spectrum antifungal activity (79). Third, several hydroxyquinolines have (or have had) both topical and oral forms (for use against dandruff and scalp dermatitis, eczema, fungal skin infections, and infectious diarrhea caused by protozoa or Shigella bacteria) suggesting that hydroxyquinolines might be effective against both internal and skin-based infections. Finally, the hydroxyquinolines are of interest because, as shown here, *C. auris* develops only mild resistance, despite long-term exposure in our experiments. The roughly twofold- to fivefold increases in resistance we observed remain well below the minimum toxicities seen for human cells and are significantly less than the 30- to 500-fold increases in resistance reported for similar studies with fluconazole or caspofungin, two of the most widely used antifungal drugs (55–57). Furthermore, hydroxyquinoline resistance resulted in only modest, if any, increases in resistance to other antifungal agents, and it led to increased susceptibility to at least one antifungal agent in common use, posaconazole. The possibility exists that a combination treatment involving a hydroxyquinoline and posaconazole might leave *C. auris* trapped between increasing *CDR1* expression to resist posaconazole, becoming more susceptible to the hydroxyquinoline, or decreasing *CDR1* expression to resist the hydroxyquinoline, becoming more susceptible to posaconazole, a hypothesis that is amenable to testing in animal models and in culture.

When considering repurposing the hydroxyquinolines as a treatment for *C. auris*, it is important to note that an oral version of clioquinol was withdrawn from usage as an antiparasitic in the early 1970s following a report associating it with an outbreak of subacute myelo-optic neuropathy (SMON) in Japan (80–83). Since that time, however, the data in the report linking SMON and clioquinol have been questioned; it has been noted that similar associations did not occur in countries with higher clioquinol usage at the time and that many of the patients developing SMON had not taken clioquinol prior to the onset of symptoms (84, 85). As such, there has been recent interest in using clioquinol to treat both Alzheimer's disease and cancer (58, 76, 80, 81, 86–89). The work reported here suggests that clioquinol and its derivatives could also be developed as effective antifungal agents, particularly against the emerging pathogen *C. auris*.

Although our results are consistent with the idea that 8-hydroxyquinolines may be able to be repurposed as a treatment for *C. auris* (along with other *Candida* species), several considerations remain to be addressed. First, our resistance study was focused on *C. auris* strains that were resistant to one or more traditional antifungal agents. There remains the possibility that more susceptible *C. auris* strains might develop different mechanisms of resistance to clioquinol. Given the scale of these experiments (three cultures from two strains), it is also possible that other potential resistance mechanisms could arise even in those strains we tested (e.g., hyperactive mutations of *MRR1*). The second major consideration relates to the therapeutic indexes observed for the 8-hydroxyquinolines. A therapeutic index of 10, or five in the case of the evolved resistant strains, is not optimal and raises questions about the use of this family of compounds in the host. We note, however, that the therapeutic indexes reported here are always the lowest value observed, representing the most conservative position possible. It has been shown that clioquinol concentrations of 13 to 25 µM in serum are achievable for several months with few or no side effects (90); this would correspond to a therapeutic index of 20 to 200 (or even wider). The third major consideration relates to the mitigation of clioquinol's effect when metals, especially iron, are present at high concentrations in the growth medium. As the concentration of iron has been reported to be as high as 25 mM in the gut in a rat model (91), this raises the possibility that physiological iron concentrations in some host niches could render clioquinol (and other 8-hydroxyquinolines) ineffective. It is important to note, however, that the same study found that only a small portion of iron, 0.4 mM, was freely available in solution (91). Furthermore, the aforementioned clioquinol serum concentrations were achieved through oral dosing (90), suggesting that free iron in the gut does not present an insurmountable barrier. In regards to both the second and third concerns, it is important to note that multiple 8-hydroxyquinolines have established abilities to treat bacterial, fungal, and parasitic infections in a number of contexts (e.g., topical and internal usage); this indicates that neither the low therapeutic indexes nor inhibition by iron should, *a priori*, be used to rule out the potential for this family to be used as part of a *C. auris* treatment regime. Consistent with this, we note that the related hydroxyquinoline nitroxoline (which had an IC_{50} of 1.6 to 3.6 µM against *C. auris* in our SAR studies) has recently been reported to be effective at treating granulomatous amebic encephalitis caused by the amoeba *Balamuthia mandrillaris* (92). Finally, although general effects associated with clioquinol treatment have been reported [e.g., metal starvation and/or abnormal metal storage (58, 75, 76)], we wish to stress that we do not know the detailed mechanism of action for this family of compounds against *C. auris*. Further work to discern the mechanism of action could lead to a deeper understanding of mechanisms of resistance, the identification of vulnerabilities in fungal defenses, and the development of more effective compounds in the 8-hydroxyquinoline class.

MATERIALS AND METHODS

Drug libraries

The primary screen in this study used both the Selleck Chem FDA-Approved Drug Library (#L1300, 1,591 compounds) and the Medicines for Malaria Venture Pandemic Response Box (399 compounds). Details about the sources of drugs for subsequent assays can be found in File S2.

Media

Cells were allowed to recover from glycerol stocks for at least 2 days at 30°C on yeast extract peptone dextrose (YEPD) plates (2% Bacto peptone, 2% dextrose, 1% yeast extract, 2% agar). Unless otherwise noted, overnight cultures for assays, recovery dilutions, and assays were performed in Roswell Park Memorial Institute (RPMI)-1640 media (containing L-glutamine and lacking sodium bicarbonate, MP Biomedicals

#0910601) supplemented with 34.5 g/L MOPS (Sigma M3183) and adjusted to pH 7.0 with sodium hydroxide before sterilizing with a 0.22 µm filter.

Strains

A full list of strains used in this study can be found in File S2. Twelve of the 13 *C. auris* isolates used in this study were acquired from the Centers for Disease Control and Prevention's Antibiotic Resistance Isolate Bank *Candida auris* panel (https://wwwn.cdc.gov/ARIsolateBank/Panel/PanelDetail?ID=2). The remaining *C. auris* isolate was a previously reported isolate from a patient at UCSF; this strain is a member of clade I that has some resistance to fluconazole (MIC 32 µg/mL) and was provided by the UCSF Clinical Laboratories at China Basin (93), this strain is available from us upon request. For *C. albicans* (SC5314), *Candida dubliniensis* (CD36), and *Candida glabrata* (CBS138), we used the sequenced strains SC5314, CD36, and CBS138/ATCC 2001, respectively. SC5314 was isolated from a patient with disseminated candidiasis prior to 1968 (94–97), CD36 was isolated from the mouth of an Irish HIV patient between 1988 and 1994 (98), and CBS138 is listed as coming from a fecal sample (https://www.atcc.org/products/all/2001.aspx#history). Unless otherwise noted, assays used the same three *C. auris* isolates (AR-384/MLY1540, clade III; AR-386/MLY1542, clade IV; AR-387/MLY1543, clade I) to ensure representation of the three clades most associated with serious infections as well as wide distribution of susceptibilities to fluconazole and caspofungin. A fourth isolate, AR-390/MLY1546 from clade I was included as the second strain, in addition to AR-384/MLY1540, in the experimental evolution experiment.

A full list of oligonucleotides and plasmids used for the construction of strains can be found in File S2. Strain construction took place in the AR-387 and AR-390 *C. auris* strain backgrounds following previously described methods using the hygromycin B resistance selectable marker (99). gRNA was designed using the gRNA selection tool in Benchling with the following parameters: "Single guide," "Guide Length" of 20, "PAM" of NGG with the *C. auris* B8441 (AR-387) reference genome. The gRNA fragments were amplified from pCE41 while the Cas9 construct was prepared by digesting pCE38 with the restriction enzyme MssI. The repair template was created by amplifying genomic DNA and amplicons were subsequently stitched together with an additional round of PCR cycling to create full-length repair template integrating the desired mutation or deletion. When constructing a gene deletion strain, a unique 23 bp ADDTAG (CGAGACGAGTGCTCGACATGAGG), which includes a 20 bp gRNA recognition sequence and PAM, was inserted at the location of the gene for any subsequent downstream edits at this locus (100, 101). Synonymous and non-synonymous mutations were introduced using the PCR stitching method and the mutations are denoted by lowercase letters in the oligo sequences described in File S2. The protospacer adjacent motif (PAM) NGG and gRNA recognition sequence were mutated to ablate further cutting by Cas9. Transformations used a lithium acetate competence/heat shock-based protocol with a 4-h recovery before plating on yeast extract-peptone dextrose (YPD) + hygromycin (HYG) 600. Potentially successful transformations were verified by colony PCR. In order to confirm the presence of desired mutations, DNA for sequencing was extracted using a Quick-DNA Fungal/Bacterial Miniprep Kit (Zymo Research D6005) coupled with a Mini-BeadBeater 16 (Biospec Products); bead beating consisted of two 4-min cycles separated by a 5-min incubation on ice.

Antifungal susceptibility testing

Antifungal susceptibility testing assays were performed as follows. Overnight cultures (3 mL, in test tubes) were started in RPMI-1640 media on a roller drum at 30°C from 2- to 3-day-old colonies grown on YPD agar plates. The following morning, the OD_{600} of the overnight cultures was determined, cultures were diluted back to OD_{600} = 0.25 in fresh RPMI-1640, and the diluted cultures were allowed to recover at 30°C for at least 3 h. After the recovery growth step, the OD_{600} of the recovery cultures was determined and the cells were diluted to an OD_{600} = 0.00357 in fresh RPMI-1640. Adding of 21 µL of the

OD_{600} = 0.00357 resuspension to 54 µL of media/drug mixture in each well resulted in a starting density of OD_{600} = 0.001 or approximately 1×10^4 cells/mL.

Fifty-four microlitres of media was dispensed into wells (in two 27 µL steps) using a BioMek FX (Beckman-Coulter). Drugs, DMSO loading controls, and other compounds (e.g., metals) were then dispensed into the media using a Labcyte Echo 525. The 21 µL of cell solution was then added to the 54 µL of media/drug mixture using a BioMek FX. Assays were performed in transparent, sterile, flat-bottomed, non-tissue culture treated 384-well microtiter plates (Thermo 242765 or 242757) that were sealed with Breathe-Easy sealing membranes (Diversified Biotech, BEM-1) immediately following inoculation. Plates were then incubated at 35°C in a humidified incubator (with 0.1% CO_2) for 24 h. After the 24-h incubation, the absorbance (OD_{600}) was determined on a prewarmed (35°C) Tecan Spark10M, taking one read per well. In all experiments, the percent inhibition was determined by first subtracting the background OD_{600} (culture wells filled with media only) from the test well OD_{600}, and then normalizing to the average OD_{600} of untreated (vehicle only) control wells cultured side-by-side with the test wells. The percent inhibition was then calculated using the following equation: % inhibition = 100 × [1 − (test well OD − background OD)/(untreated control OD − background OD)].

Primary screening

Initial screening was conducted with the three primary *C. auris* strains. All 1,990 screening compounds were evaluated for *in vitro* efficacy at concentrations of 1 and 10 µM. For each of the strains, a single well was evaluated for each compound at each concentration. The efficacy of each compound was determined by comparison to the average of untreated control wells on the same culture plate as the tested compounds. Compounds with greater than 50% inhibition of *C. auris* growth for at least two of the three tested strains and a B-score [a non-control based method for systematic error correction which accounts for position effects, see references (50, 51) for further details] greater than 0.1 were selected as hits for further evaluation (86 compounds total). The raw data for this experiment are included in File S3.

Secondary drug screening and IC_{50} determinations

The activity of 86 primary hit compounds was validated against the three primary *C. auris* strains with dose-response growth inhibition experiments. Drugs were dispensed into test wells using the Labcyte Echo 525 liquid handler to generate 8-point concentration ranges from 0.3 to 100 µM. All drugs were resuspended in DMSO and compared to appropriate vehicle-only controls. Dose-response experiments were performed with two biological replicates, each consisting of two technical replicates. Half maximal inhibitory concentrations (IC_{50}s) were calculated from dose-response curves generated in GraphPad Prism 7 using four parameter logistic regression. Extreme outliers were removed from analysis to facilitate curve fitting; these outliers were most commonly associated with drug precipitation although some may reflect the Eagle effect. The raw data for this experiment are included in File S4.

Subsequent experiments determined the IC_{50}s of the top five hit drugs as well as four standard-of-care drugs against 13 different *C. auris* strains, as well as one strain each of *C. albicans*, *C. glabrata*, and *C. dubliniensis* with 22-point dose-response ranges (0.05–2,600 µM for fluconazole; 0.001–133.3 µM for caspofungin, miltefosine, and triclabendazole; 0.001–20 µM for posaconazole, amphotericin B, chloroxine, broxyquinoline, and clioquinol) performed as described above with three biological replicates, each consisting of two technical replicates. After background correction, data from all three biologic replicates were pooled and used to generate dose-response curves in R Studio (version 1.2.5033). The IC_{50} including the 95% confidence interval was calculated using an N-parameter logistic regression model for each drug (library: nplr version 0.1.7). Ggplot2 (version 3.2.1) was used to generate forest plots of the IC_{50} (95% confidence interval) for each strain as well as the LD50 (95% confidence interval) of three human

cell lines with the lower limit of the lethal dose highlighted in red. The scripts and raw data used in this analysis are available at www.github.com/srlevan in the "Lohse_CAuris_2023" repository.

Human cell toxicity measurements

The human cell lines Hep-G2 (liver), HEK-293 (kidney), and HFF-1 (fibroblast) were cultured in Dulbecco's modified Eagle's medium (Gibco) containing 10% (vol/vol) fetal bovine serum (Gibco), 2 mM l-glutamine, 100 U/mL penicillin/streptomycin (Gibco), and 10 mM 4-(2-hydroxyethyl)-1-piperazineethanesulfonic acid (HEPES) buffer. For toxicity experiments, all human cell lines were seeded into sterile, opaque 384-well culture plates (Corning 3570) 1 day prior to drug addition. Drugs were added using the Labcyte Echo 525 liquid handler to generate 22-point dose-response concentration ranges. Cells were cultured in the presence of drug for 72 h prior to addition of CellTiter-Glo 2.0 reagent (Promega) and collection of luminescence values in relative luminescence units (RLU) using the Promega GloMax plate reader. The percent viability of each treated culture was calculated using the following equation: % inhibition = 100 × (test well RLU)/(untreated control RLU). IC_{50} values for each drug against human cell lines were calculated as described above. Toxicity experiments were performed with three biological replicates, each consisting of two technical replicates.

Drug susceptibility in evolved and genetically engineered *C. auris* strains

C. auris strains selected for clioquinol resistance or engineered for specific mutations were generated and cultured as described previously and the IC_{50} of clioquinol and other drugs was determined as described above using 15-point dose-response ranges (0.1–20 µM for clioquinol; 3.3–1,333 µM for fluconazole; 0.03–66.7 µM for broxyquinoline and amphotericin B; 0.003–13.3 µM for posaconazole, voriconazole, and micafungin). All strains were tested simultaneously for direct comparison of drug effects and three biological replicates were performed, each consisting of two technical replicates. Fold-changes in IC_{50} were calculated relative to the parental strains from which each mutant strain was derived.

SAR assays

A group of 32 commercially available drugs or compounds that are structurally related to clioquinol were selected for SAR experiments. All drugs were resuspended in DMSO and tested for inhibition of the three primary *C. auris* strains with 15-point dose-response ranges from 0.01 to 150 µM. Experiments were performed and IC_{50} values were calculated as described above with three biological replicates, each consisting of two technical replicates. As with the verification screen, extreme outliers from this experiment were removed from analysis to facilitate curve fitting. The raw data for this experiment are included in File S5.

Metal supplementation experiments

Stock 10 mM metal solutions for supplementation experiments were prepared in sterile water as follows: Ca^{2+} solution from calcium chloride (Sigma C79-500); Mg^{2+} solution from magnesium sulfate (Sigma 246972); Fe^{2+} solution from ferrous(II) sulfate (Sigma F8048); Fe^{3+} solution from ferric(III) chloride (Sigma F-2877); Cu^{2+} solution from copper(II) sulfate (Sigma C7631); Mn^{2+} solution from manganese sulfate (Sigma M-1144); Zn^{2+} solution from zinc sulfate (Sigma 96500). For metal supplementation experiments, *C. auris* was grown in RPMI media depleted of divalent metal ions using Chelex 100 resin (Biorad) following the manufacturer's protocol. Drugs and metals were dispensed into culture wells using the Labcyte Echo 525 liquid handler prior to addition of *C. auris* cells. Ethylenediaminetetraacetic acid (EDTA) and *N*,*N*,*N*′,*N*′-tetrakis(2-pyridinylmethyl)−1,2-ethanediamine (TPEN) were used as control chelating agents for comparison to antifungal drugs. The percent inhibition for each drug/metal condition was

calculated as described above. For calculation of clioquinol IC_{50} in the context of different metal concentrations, 8-point dose-responses ranges from 0.01 to 10 µM were used. Experiments were performed with three biological replicates, each consisting of two technical replicates.

Viability determination by plating

Viability assays were performed using the AR-384 strain. In brief, overnight cultures (3 mL, in test tubes) were started in RPMI-1640 media on a roller drum at 30°C from 2- to 3-day-old colonies grown on YPD agar plates. The following morning, the OD_{600} of the overnight cultures was determined, cultures were diluted back to OD_{600} = 0.7 in 8 mL fresh RPMI-1640, and the diluted cultures were allowed to recover at 30°C for 3 h. After 3 h, clioquinol (5 µM) and DMSO controls were added to the cultures which were then incubated overnight on a roller drum at 30°C. As a positive control for cell death, an independent culture was pelleted and resuspended in 70% isopropanol for 1 h at room temperature (roughly 20 to 22°C) with vortexing every 15 min. Aliquots were taken from the 22-h clioquinol and DMSO treated cultures as well as 1 h isopropanol treated cultures, cells were PBS washed, and preliminary 10× stocks of normalized cell density were created based on OD_{600}. The cell density of each sample was then determined by flow cytometry using a BD Accuri C6 Plus; cell counts were based on the number of cells detected in a 10 µL sample. 1× normalized cell density stocks were then created based on these measurements. The exact cell density of these 1× stocks was then determined by flow cytometry of 10 µL of each solution. Next, both high-density (1:20 dilution) and low-density (1:200 dilution) stocks were made from the 1× stock and plated (50 µL of high density, 60 µL of low density) on YEPD plates at 30°C. Three low-density and two high-density plates were used for clioquinol and DMSO samples; two low- and one high-density plates were used for isopropanol samples. After 2 days, colony numbers were determined using a Protos 3 (Synbiosis) automated colony counter. The input cell density (cells/µL) and detectable colonies (CFU) were both normalized to their respective DMSO treated samples and normalized viability (relative to the DMSO treated samples) was determined by dividing the normalized CFU for each sample by the normalized input cell density.

Iron supplementation recovery assay

Iron supplementation recovery assays were performed on the AR-384 strain and flow cytometry for the iron supplementation recovery assays was performed on the previously described BD Accuri C6 Plus. Overnight cultures (3 mL, in test tubes) were started in RPMI-1640 media on a roller drum at 30°C from 2- to 3-day-old colonies grown on YPD agar plates. The following morning, the OD_{600} of the overnight cultures was determined, cultures were diluted back to OD_{600} = 0.5 in fresh RPMI-1640, and the diluted cultures were allowed to recover at 30°C for 3 h at which point 4 µM clioquinol was added to the cultures. Cultures were then incubated a further 21 h on a roller drum at 30°C. After the 21-h incubation, two 1 mL aliquots were pulled from each clioquinol treated sample and either iron [2 µM each of iron (II) sulfate and iron (III) chloride] or water (equivalent volumes to the iron solutions) was added. Four clioquinol samples were processed in this way. The density of each culture was then determined by flow cytometry and the strains were incubated on a roller drum at 30°C for 25 h. At each subsequent time point, the cultures were vortexed after which samples were removed and diluted with D-PBS. The cell density of each sample was then determined by flow cytometry; cell counts were based on the number of cells detected in a 10 µL sample.

Liquid resistance assay

Two overnights of AR-384 and one of AR-390 were started from independent single colonies, the following morning the overnight cultures were diluted back to OD_{600} = 0.05 in fresh media and allowed to recover for 3 h. At this point, clioquinol was added

to the cultures at 0.75 µM (AR-384) or 0.4 µM (AR-390), and the cultures were incubated for 2 days on a roller drum at 30°C. Samples were then diluted back to approximately OD_{600} = 0.01 in the presence of fresh media and drug. The three independent cultures were passaged a further 30 times in this manner with passages occurring every 3 days, rather than every 2 days after passage 20 (we note that samples were frozen down after passage 20, passage 21 was started from single colonies on plates made from these frozen stocks). Clioquinol concentrations were slowly increased during the course of the experiment in response to increased growth by strains; see File S6 for the clioquinol concentration present for each passage. In parallel to this experiment, 18 passages were made of two independent control cultures for each strain where equivalent volumes of DMSO were added at each passage.

RT-qPCR methods

Three independent overnight cultures for each strain were started from independent single colonies on roller drum at 30°C, the following morning the overnight cultures were diluted back to OD_{600} = 0.35 in 5 mL fresh media and allowed to recover for 6 h. We note that clioquinol was not present in the overnight or recovery cultures and as such these samples reflect the basal, as opposed to clioquinol-induced, expression levels. Cultures were then spun down, decanted, and the pellets flash frozen with liquid nitrogen before storage at −80°C. Pellets were thawed and RNA was extracted using the MasterPure Yeast RNA Purification Kit (Lucigen MPY03100) followed by DNase treatment with the DNase TURBO DNA-free kit (Invitrogen AM1907). RNA was diluted 1:50 for RT-qPCR which was conducted using the Luna Universal One-Step RT-qPCR kit (New England Biolabs E3005E) on a C1000 touch thermal Cycler/CFX384 Real-Time System (Biorad). Reactions were performed in Hard-Shell PCR Plates (384 well, thin-wall, Biorad HSP3805) sealed with Microseal B Adhesive Sealers (Biorad MSB-1001). Two independent oligonucleotide sets each were used for *CDR1*, *CDR2*, and *MDR1*; one of the *CDR1* oligonucleotide sets was located downstream of the E772* mutation. One oligonucleotide set each was used for the control genes *UBC4* and *ACT1*. Two technical replicates were performed for each oligonucleotide set for each biological replicate. The Cq values for the two technical replicates were averaged for each set, after which the averaged Cq values for the *UBC4* and *ACT1* sets for each biological replicate were then averaged. The ΔCt was then determined for each primer set versus the averaged *UBC4*/*ACT1* Cq, after which the ΔΔCt was calculated versus the parental strain, and the fold change was determined by taking 2^(−ΔΔCt). The average was then calculated for the two probe sets for each gene within each biological replicate, after which the average and standard deviation were calculated for each gene across the three biological replicates.

DNA sequencing

For endpoint samples of the evolved strains, two cultures were inoculated from independent single colonies (single colony samples) and a third culture was started from the dense portion of the streak on the plate (population samples). For samples from intermediate time points for the evolved strains, single cultures were started from the dense portion of the streak on the plate (population samples). A single culture was inoculated from an independent colony for the parental strains. One culture was inoculated from an independent colony (single colony samples) and a second culture was started from the dense portion of the streak on the plate (population samples) for the DMSO control cultures. Cultures for whole genome DNA sequencing were grown in 8 mL media overnight on a roller drum at 30°C. Prior to harvesting the following morning, a sample was pulled to freeze as a glycerol stock for future use. 6.2 mL of each culture was spun down, decanted, flash frozen in liquid nitrogen, and stored at −80°C.

DNA was extracted using the Quick-DNA Fungal/Bacterial Miniprep Kit (Zymo Research D6005) with two 5-min cycles on a TissueLyser II (Qiagen) separated by a 5-min incubation on ice; final elution was in 60 µL water and concentrations were determined

on a Nanodrop 2000c (Thermo Scientific). The DNA was diluted to 100 µL at a concentration of 10 ng/µL and then sheared using a Biorupter Pico (Diagenode) with 13 cycles of 30 s on followed by 30 s off and quantified using an Agilent D1000 ScreenTape (Agilent Technologies); DNA fragment size after this step averaged 240 bp.

Library preparation was performed using the NEBNext Ultra DNA Library Prep Kit for Illumina (E7370), using the 200 bp recommended bead volumes for step 3, 5 PCR cycles for step 4, and eluting in water for step 5. See File S6 for a list of the i7_index_RC and i5_index_RC oligonucleotides used for each sample. Eluted libraries for sequencing were then quantified via Qubit, pooled, the pooled mixture quantified via Qubit, and then the pooled libraries were quantified using an Agilent High Sensitivity D1000 ScreenTape (Agilent Technologies); DNA fragment size after this step averaged 360 bp.

Sequencing was performed by the Chan Zuckerberg Biohub Genomics Platform on an Illumina NextSeq 550 using a NextSeq 500/550 v2.5 reagent kit (300 cycles, 150 bp paired end read, 12 bp index length for reads 1 and 2). The number of reads per sample varied between 8,621,624 and 18,340,887 (File S6). Sequences were aligned to the reference genomes using Bowtie2 (v 2.4.4) with default settings, the overall alignment rate varied between 89.38% and 94.57% (File S6), for an approximate sequencing depth ranging from 95× to 200× with an average of 150×. AR-390 based strains were aligned to B8441 chromosome FASTA and GFF features files from the *Candida* Genome Database (version s01-m01-r-17, dating from 8 August 2021, downloaded on 10 September 2021). AR-384 based strains were aligned to B11221 chromosome FASTA and GFF features files from the *Candida* Genome Database (no version information, dating from 17 December 2019, downloaded on 10 September 2021). Aligned reads were then filtered using Samtools (version 1.13) to remove reads with a Cigar Value of "*." Mutations in genes were identified using Minority Report (version 1.0, available at https://github.com/JeremyHorst/MinorityReport) (102) in Python 2 (version 2.7.15) with the parental AR-384 and AR-390 sequencing reads used as the basis for comparison, the analyze "Copy Number Variants" (CNV) feature was enabled, and the codon table changed to reflect the use of "CTG" as serine rather than leucine. For single colony samples, the default settings were used; these settings identified mutations that were present in at least 90% of the population. For population samples, CNV analysis was conducted and the following settings were used:
"vp" (minimum_variant_proportion) of 0.1, "wp" (maximum_variant_proportion) of 0.04, "vc" (minimum_variant_counts) of 10, and "wc" (maximum_wildtype_variant_counts) of 50. In other words, a mutation or variant must be present in at least 10% of experimental sample reads with a minimum requirement for 10 reads and must be present in no more than 4% of parental sequencing reads with a maximum limit of 50 reads. The Minority Report output files for each sample can be found in File S6. As a parallel approach, variant sequences were identified from the alignment sam files which were filtered for map quality using Samtools (version 1.13) and BCFtools (version 3.6.3) (103) with the output organized from the VCF files using R (104) with extensive use of *tidyverse* (105). The position of each variant was determined to be within a gene (or in an intergenic region) based on coordinates from GFF files, considering "gene" features, which include introns. The results of this analysis are also included in File S6 and the scripts used to perform this analysis are available at www.github.com/srlevan in the "Lohse_CAuris_2023" repository. Additional details explaining the Minority Report and alternative R-based mutation identification outputs are provided in File S7.

ACKNOWLEDGMENTS

We thank the Centers for Disease Control and Prevention's Antibiotic Resistance Isolate Bank and UCSF's Clinical Laboratories at China Basin for strains. We thank Ananda Mendoza for technical support.

This work was supported by NIH grants R01AI049187 (to A.D.J.), R35GM124594 (to C.J.N.), and an NIH Fellowship F31DE028488 (to C.L.E) and by the Kamangar family in the form of an endowed chair (to C.J.N.). M.T.L. and J.L.D. were supported by the Chan

Zuckerberg Biohub. The content is the sole responsibility of the authors and does not represent the views of the NIH or other funding agencies. Neither the NIH nor other funding agencies had any role in the design of the study, in the collection, analyses, or interpretation of data, in the writing of the manuscript, or in the decision to publish the results.

AUTHOR AFFILIATIONS

[1]Department of Microbiology and Immunology, University of California, San Francisco, California, USA
[2]Department of Biochemistry and Biophysics, University of California, San Francisco, California, USA
[3]Department of Medicine, University of California, San Francisco, California, USA
[4]Department of Molecular and Cell Biology, School of Natural Sciences, University of California, Merced, California, USA
[5]Quantitative and Systems Biology Graduate Program, University of California, Merced, California, USA
[6]Health Sciences Research Institute, University of California, Merced, California, USA
[7]Chan Zuckerberg Biohub, San Francisco, California, USA

PRESENT ADDRESS

Craig L. Ennis, Graphite Bio, San Francisco, California, USA

AUTHOR ORCIDs

Matthew B. Lohse http://orcid.org/0000-0002-1071-781X
Clarissa J. Nobile http://orcid.org/0000-0003-0799-6499

FUNDING

Funder	Grant(s)	Author(s)
HHS | NIH | National Institute of Allergy and Infectious Diseases (NIAID)	R01AI049187	ALEXANDER D JOHNSON
HHS | NIH | National Institute of General Medical Sciences (NIGMS)	R35GM124594	Clarissa J Nobile
HHS | National Institutes of Health (NIH)	F31DE028488	Craig L Ennis
Chan Zuckerberg Initiative (CZI)		Joseph L DeRisi
Kamangar Family		Clarissa J Nobile

AUTHOR CONTRIBUTIONS

Matthew B. Lohse, Conceptualization, Data curation, Formal analysis, Methodology, Resources, Validation, Visualization, Writing – original draft, Writing – review and editing, Investigation | Matthew T. Laurie, Conceptualization, Data curation, Formal analysis, Investigation, Methodology, Resources, Validation, Visualization, Writing – original draft, Writing – review and editing | Sophia Levan, Data curation, Formal analysis, Investigation, Methodology, Resources, Validation, Visualization, Writing – original draft, Writing – review and editing | Naomi Ziv, Data curation, Formal analysis, Investigation, Validation, Writing – review and editing | Craig L. Ennis, Methodology, Resources, Writing – review and editing | Clarissa J. Nobile, Resources, Writing – review and editing, Funding acquisition, Supervision | Joseph DeRisi, Conceptualization, Formal analysis, Writing – review and editing, Funding acquisition, Supervision, Project administration | Alexander D. Johnson, Conceptualization, Formal analysis, Writing – review and editing, Funding acquisition, Supervision, Project administration

DATA AVAILABILITY

Data from the Illumina sequences analyzed for this project are available at the NCBI Sequence Read Archive (SRA) as BioProject accession number PRJNA932032 (biosamples SAMN33143520 through SAMN33143533; SRA experiments SRR23353631 through SRR23353654).

ADDITIONAL FILES

The following material is available online.

Supplemental Material

File S1 (mBio01376-23-S0001.xlsx). Summary data related to Figures 1B, 2A, 2B, and 4A.
File S2 (mBio01376-23_S0002.xlsx). Compiled information relating to strains, plasmids, oligonucleotides, and compounds used in this study.
File S3 (mBio01376-23_S0003.xlsx). Plate guide, plate maps, and raw data for the 1,990 compound primary screen, associated with Figure 1B.
File S4 (mBio01376-23_S0004.xlsx). Plate guide, plate maps, and raw data for the 86 compound secondary screen, associated with Figure 2A.
File S5 (mBio01376-23_S0005.xlsx). Plate guide, plate maps, and raw data for the structure-activity relationship (SAR) screen, associated with Figure 4A.
File S6 (mBio01376-23_S0006.xlsx). Compiled information and results relating to experimental evolution strain sequencing.
File S7 (mBio01376-23_S0007.docx). Supplemental text explaining the Minority Report and alternative R-based mutation identification outputs.
Figure S1 (mBio01376-23_S0008.pdf). Clioquinol is fungistatic to *C. auris*.

REFERENCES

1. Fraser VJ, Jones M, Dunkel J, Storfer S, Medoff G, Dunagan WC. 1992. Candidemia in a tertiary care hospital: epidemiology, risk factors, and predictors of mortality. Clin Infect Dis 15:414–421. https://doi.org/10.1093/clind/15.3.414
2. Forsberg K, Woodworth K, Walters M, Berkow EL, Jackson B, Chiller T, Vallabhaneni S. 2019. *Candida auris*: the recent emergence of a multidrug-resistant fungal pathogen. Med Mycol 57:e7. https://doi.org/10.1093/mmy/myy156
3. Schelenz S, Hagen F, Rhodes JL, Abdolrasouli A, Chowdhary A, Hall A, Ryan L, Shackleton J, Trimlett R, Meis JF, Armstrong-James D, Fisher MC. 2016. First hospital outbreak of the globally emerging *Candida auris* in a European hospital. Antimicrob Resist Infect Control 5:35. https://doi.org/10.1186/s13756-016-0132-5
4. Eyre DW, Sheppard AE, Madder H, Moir I, Moroney R, Quan TP, Griffiths D, George S, Butcher L, Morgan M, Newnham R, Sunderland M, Clarke T, Foster D, Hoffman P, Borman AM, Johnson EM, Moore G, Brown CS, Walker AS, Peto TEA, Crook DW, Jeffery KJM. 2018. A *Candida auris* outbreak and its control in an intensive care setting. N Engl J Med 379:1322–1331. https://doi.org/10.1056/NEJMoa1714373
5. Pacilli M, Kerins JL, Clegg WJ, Walblay KA, Adil H, Kemble SK, Xydis S, McPherson TD, Lin MY, Hayden MK, Froilan MC, Soda E, Tang AS, Valley A, Forsberg K, Gable P, Moulton-Meissner H, Sexton DJ, Jacobs Slifka KM, Vallabhaneni S, Walters MS, Black SR. 2020. Regional emergence of *Candida auris* in Chicago and lessons learned from intensive follow-up at 1 ventilator-capable skilled nursing facility. Clinical Infectious Diseases 71:e718–e725. https://doi.org/10.1093/cid/ciaa435
6. Rossow J, Ostrowsky B, Adams E, Greenko J, McDonald R, Vallabhaneni S, Forsberg K, Perez S, Lucas T, Alroy KA, Jacobs Slifka K, Walters M, Jackson BR, Quinn M, Chaturvedi S, Blog D, New York Candida auris Investigation Workgroup. 2021. Factors associated with *Candida auris* colonization and transmission in skilled nursing facilities with ventilator units, New York, 2016-2018. Clin Infect Dis 72:e753–e760. https://doi.org/10.1093/cid/ciaa1462
7. Southwick K, Ostrowsky B, Greenko J, Adams E, Lutterloh E, NYS C. auris Team, Denis RJ, Patel R, Erazo R, Fernandez R, Bucher C, Quinn M, Green C, Chaturvedi S, Leach L, Zhu Y. 2022. A description of the first *Candida auris*-colonized individuals in New York state, 2016-2017. Am J Infect Control 50:358–360. https://doi.org/10.1016/j.ajic.2021.10.037
8. Allaw F, Kara Zahreddine N, Ibrahim A, Tannous J, Taleb H, Bizri AR, Dbaibo G, Kanj SS. 2021. First *Candida auris* outbreak during a COVID-19 pandemic in a tertiary-care center in Lebanon. Pathogens 10:157. https://doi.org/10.3390/pathogens10020157
9. Prestel C, Anderson E, Forsberg K, Lyman M, deMA, Kuhar D, Edwards K, Rivera M, Shugart A, Walters M, Dotson NQ. 2020. *Candida auris* outbreak in a COVID-19 specialty care unit. MMWR Morb Mortal Wkly Rep 70:56–57. https://doi.org/10.15585/mmwr.mm7002e3
10. Centers for disease control and prevention. 2020. Available from: https://www.cdc.gov/fungal/candida-auris/c-auris-alert-09-17.html
11. 2022. WHO fungal priority pathogens list to guide research, development and public health action. World Health Organization.
12. Satoh K, Makimura K, Hasumi Y, Nishiyama Y, Uchida K, Yamaguchi H. 2009. *Candida auris* SP. Nov., a novel Ascomycetous yeast isolated from the external ear canal of an inpatient in a Japanese hospital. Microbiol Immunol 53:41–44. https://doi.org/10.1111/j.1348-0421.2008.00083.x
13. Lockhart SR, Etienne KA, Vallabhaneni S, Farooqi J, Chowdhary A, Govender NP, Colombo AL, Calvo B, Cuomo CA, Desjardins CA, Berkow EL, Castanheira M, Magobo RE, Jabeen K, Asghar RJ, Meis JF, Jackson B, Chiller T, Litvintseva AP. 2017. Simultaneous emergence of multidrug-resistant *Candida auris* on 3 continents confirmed by whole-genome sequencing and epidemiological analyses. Clin Infect Dis 64:134–140. https://doi.org/10.1093/cid/ciw691
14. Chow NA, de Groot T, Badali H, Abastabar M, Chiller TM, Meis JF. 2019. Potential fifth clade of *Candida auris*, Iran, 2018. Emerg Infect Dis 25:1780–1781. https://doi.org/10.3201/eid2509.190686
15. Muñoz JF, Gade L, Chow NA, Loparev VN, Juieng P, Berkow EL, Farrer RA, Litvintseva AP, Cuomo CA. 2018. Genomic insights into multidrug-resistance, mating and virulence in *Candida auris* and related emerging species. 1. Nat Commun 9:5346. https://doi.org/10.1038/s41467-018-07779-6

16. Chow NA, Muñoz JF, Gade L, Berkow EL, Li X, Welsh RM, Forsberg K, Lockhart SR, Adam R, Alanio A, Alastruey-Izquierdo A, Althawadi S, Araúz AB, Ben-Ami R, Bharat A, Calvo B, Desnos-Ollivier M, Escandón P, Gardam D, Gunturu R, Heath CH, Kurzai O, Martin R, Litvintseva AP, Cuomo CA. 2020. Tracing the evolutionary history and global expansion of *Candida auris* using population genomic analyses. mBio 11:e03364-19. https://doi.org/10.1128/mBio.03364-19
17. Kwon YJ, Shin JH, Byun SA, Choi MJ, Won EJ, Lee D, Lee SY, Chun S, Lee JH, Choi HJ, Kee SJ, Kim SH, Shin MG. 2019. *Candida auris* clinical isolates from South Korea: identification, antifungal susceptibility, and genotyping. J Clin Microbiol 57:e01624-18. https://doi.org/10.1128/JCM.01624-18
18. Welsh RM, Sexton DJ, Forsberg K, Vallabhaneni S, Litvintseva A. 2019. Insights into the unique nature of the East Asian clade of the emerging pathogenic yeast *Candida auris*. J Clin Microbiol 57:e00007-19. https://doi.org/10.1128/JCM.00007-19
19. Chow NA, Gade L, Tsay SV, Forsberg K, Greenko JA, Southwick KL, Barrett PM, Kerins JL, Lockhart SR, Chiller TM, Litvintseva AP, US Candida auris Investigation Team. 2018. Multiple introductions and subsequent transmission of multidrug-resistant *Candida auris* in the USA: a molecular epidemiological survey. Lancet Infect Dis 18:1377–1384. https://doi.org/10.1016/S1473-3099(18)30597-8
20. Rhodes J, Fisher MC. 2019. Global epidemiology of emerging *Candida auris*. Curr Opin Microbiol 52:84–89. https://doi.org/10.1016/j.mib.2019.05.008
21. Borman AM, Johnson EM. 2020. *Candida auris* in the UK: introduction, dissemination, and control. PLoS Pathog 16:e1008563. https://doi.org/10.1371/journal.ppat.1008563
22. Chowdhary A, Prakash A, Sharma C, Kordalewska M, Kumar A, Sarma S, Tarai B, Singh A, Upadhyaya G, Upadhyay S, Yadav P, Singh PK, Khillan V, Sachdeva N, Perlin DS, Meis JF. 2018. A multicentre study of antifungal susceptibility patterns among 350 *Candida auris* isolates (2009-17) in India: role of the ERG11 and FKS1 genes in azole and echinocandin resistance. J Antimicrob Chemother 73:891–899. https://doi.org/10.1093/jac/dkx480
23. Ostrowsky B, Greenko J, Adams E, Quinn M, O'Brien B, Chaturvedi V, Berkow E, Vallabhaneni S, Forsberg K, Chaturvedi S, Lutterloh E, Blog D, C. auris Investigation Work Group. 2020. *Candida auris* isolates resistant to three classes of antifungal medications - New York, 2019. MMWR Morb Mortal Wkly Rep 69:6–9. https://doi.org/10.15585/mmwr.mm6901a2
24. Kordalewska M, Lee A, Park S, Berrio I, Chowdhary A, Zhao Y, Perlin DS. 2018. Understanding echinocandin resistance in the emerging pathogen *Candida auris*. Antimicrob Agents Chemother 62:e00238-18. https://doi.org/10.1128/AAC.00238-18
25. Zhu Y, O'Brien B, Leach L, Clarke A, Bates M, Adams E, Ostrowsky B, Quinn M, Dufort E, Southwick K, Erazo R, Haley VB, Bucher C, Chaturvedi V, Limberger RJ, Blog D, Lutterloh E, Chaturvedi S. 2020. Laboratory analysis of an outbreak of *Candida auris* in New York from 2016 to 2018: impact and lessons learned. J Clin Microbiol 58:e01503-19. https://doi.org/10.1128/JCM.01503-19
26. Kilburn S, Innes G, Quinn M, Southwick K, Ostrowsky B, Greenko JA, Lutterloh E, Greeley R, Magleby R, Chaturvedi V, Chaturvedi S. 2022. Antifungal resistance trends of *Candida auris* clinical isolates. Antimicrob Agents Chemother aac0224221. https://doi.org/10.1128/aac.02242-21
27. Kean R, Ramage G. 2019. Combined antifungal resistance and biofilm tolerance: the global threat of *Candida auris*. mSphere 4:e00458-19. https://doi.org/10.1128/mSphere.00458-19
28. Billamboz M, Fatima Z, Hameed S, Jawhara S. 2021. Promising drug candidates and new strategies for fighting against the emerging superbug *Candida auris*. Microorganisms 9:634. https://doi.org/10.3390/microorganisms9030634
29. Seiler GT, Ostrosky-Zeichner L. 2021. Investigational agents for the treatment of resistant yeasts and molds. Curr Fungal Infect Rep 15:104–115. https://doi.org/10.1007/s12281-021-00419-5
30. Aghaei Gharehbolagh S, Izadi A, Talebi M, Sadeghi F, Zarrinnia A, Zarei F, Darmiani K, Borman AM, Mahmoudi S. 2021. New weapons to fight a new enemy: a systematic review of drug combinations against the drug-resistant fungus *Candida auris*. Mycoses 64:1308–1316. https://doi.org/10.1111/myc.13277
31. Bandara N, Samaranayake L. 2022. Emerging and future strategies in the management of recalcitrant *Candida auris*. Med Mycol 60:myac008. https://doi.org/10.1093/mmy/myac008
32. Lamoth F, Lewis RE, Kontoyiannis DP. 2022. Investigational antifungal agents for invasive mycoses: a clinical perspective. Clin Infect Dis 75:534–544. https://doi.org/10.1093/cid/ciab1070
33. Giacobbe DR, Magnasco L, Sepulcri C, Mikulska M, Koehler P, Cornely OA, Bassetti M. 2021. Recent advances and future perspectives in the pharmacological treatment of *Candida auris* infections. Expert Rev Clin Pharmacol 14:1205–1220. https://doi.org/10.1080/17512433.2021.1949285
34. Berkow EL, Lockhart SR. 2018. Activity of CD101, a long-acting echinocandin, against clinical isolates of *Candida auris*. Diagn Microbiol Infect Dis 90:196–197. https://doi.org/10.1016/j.diagmicrobio.2017.10.021
35. Kovács R, Tóth Z, Locke JB, Forgács L, Kardos G, Nagy F, Borman AM, Majoros L. 2021. Comparison of *in Vitro* killing activity of Rezafungin, Anidulafungin. In Caspofungin, and micafungin against four *Candida auris* clades in RPMI-1640 in the absence and presence of human serum. microorganisms 9
36. Berkow EL, Lockhart SR. 2018. Activity of novel antifungal compound APX001A against a large collection of *Candida auris*. J Antimicrob Chemother 73:3060–3062. https://doi.org/10.1093/jac/dky302
37. Zhu Y, Kilburn S, Kapoor M, Chaturvedi S, Shaw KJ, Chaturvedi V. 2020. *In Vitro* activity of manogepix against multidrug-resistant and panresistant *Candida auris* from the New York outbreak. Antimicrob Agents Chemother 64:e01124-20. https://doi.org/10.1128/AAC.01124-20
38. Hager CL, Larkin EL, Long L, Zohra Abidi F, Shaw KJ, Ghannoum MA. 2018. *In Vitro* and *in Vivo* evaluation of the antifungal activity of APX001A/APX001 against *Candida auris*. Antimicrob Agents Chemother 62. https://doi.org/10.1128/AAC.02319-17
39. Berkow EL, Angulo D, Lockhart SR. 2017. *In Vitro* activity of a novel glucan synthase inhibitor, SCY-078, against clinical isolates of *Candida auris*. Antimicrob Agents Chemother 61:e00435-17. https://doi.org/10.1128/AAC.00435-17
40. Larkin E, Hager C, Chandra J, Mukherjee PK, Retuerto M, Salem I, Long L, Isham N, Kovanda L, Borroto-Esoda K, Wring S, Angulo D, Ghannoum M. 2017. The emerging pathogen *Candida auris*: growth phenotype, virulence factors. In Activity of Antifungals, and effect of SCY-078, a novel Glucan synthesis inhibitor, on growth morphology and Biofilm formation. Antimicrob agents Chemother 61
41. Zhu YC, Barat SA, Borroto-Esoda K, Angulo D, Chaturvedi S, Chaturvedi V. 2020. Pan-resistant *Candida auris* isolates from the outbreak in New York are susceptible to ibrexafungerp (a glucan synthase inhibitor). Int J Antimicrob Agents 55:105922. https://doi.org/10.1016/j.ijantimicag.2020.105922
42. Wiederhold NP, Najvar LK, Olivo M, Morris KN, Patterson HP, Catano G, Patterson TF. 2021. Ibrexafungerp demonstrates *in vitro* activity against fluconazole-resistant *Candida auris* and *in vivo* efficacy with delayed initiation of therapy in an experimental model of invasive candidiasis. Antimicrob Agents Chemother 65:e02694-20. https://doi.org/10.1128/AAC.02694-20
43. Chu S, Long L, Sherif R, McCormick TS, Borroto-Esoda K, Barat S, Ghannoum MA. 2021. A second-generation fungerp analog, SCY-247, shows potent *in vitro* activity against *Candida auris* and other clinically relevant fungal isolates. Antimicrob Agents Chemother 65:e01988-20. https://doi.org/10.1128/AAC.01988-20
44. Wall G, Chaturvedi AK, Wormley FL, Wiederhold NP, Patterson HP, Patterson TF, Lopez-Ribot JL. 2018. Screening a repurposing library for inhibitors of multidrug-resistant *Candida auris* identifies ebselen as a repositionable candidate for antifungal drug development. Antimicrob Agents Chemother 62:e01084-18. https://doi.org/10.1128/AAC.01084-18
45. Mamouei Z, Alqarihi A, Singh S, Xu S, Mansour MK, Ibrahim AS, Uppuluri P. 2018. Alexidine dihydrochloride has broad-spectrum activities against diverse fungal pathogens. mSphere 3:e00539-18. https://doi.org/10.1128/mSphere.00539-18
46. Wall G, Herrera N, Lopez-Ribot JL. 2019. Repositionable compounds with antifungal activity against multidrug resistant *Candida auris*

identified in the medicines for malaria venture's pathogen box. J Fungi (Basel) 5:92. https://doi.org/10.3390/jof5040092
47. de Oliveira HC, Monteiro MC, Rossi SA, Pemán J, Ruiz-Gaitán A, Mendes-Giannini MJS, Mellado E, Zaragoza O. 2019. Identification of off-patent compounds that present antifungal activity against the emerging fungal pathogen *Candida auris*. Front Cell Infect Microbiol 9:83. https://doi.org/10.3389/fcimb.2019.00083
48. Iyer KR, Camara K, Daniel-Ivad M, Trilles R, Pimentel-Elardo SM, Fossen JL, Marchillo K, Liu Z, Singh S, Muñoz JF, Kim SH, Porco JA, Cuomo CA, Williams NS, Ibrahim AS, Edwards JE, Andes DR, Nodwell JR, Brown LE, Whitesell L, Robbins N, Cowen LE. 2020. An oxindole efflux inhibitor potentiates azoles and impairs virulence in the fungal pathogen *Candida auris*. Nat Commun 11:6429. https://doi.org/10.1038/s41467-020-20183-3
49. Cheng Y-S, Roma JS, Shen M, Mota Fernandes C, Tsang PS, Forbes HE, Boshoff H, Lazzarini C, Del Poeta M, Zheng W, Williamson PR. 2021. Identification of antifungal compounds against multidrug-resistant *Candida auris* utilizing a high-throughput drug-repurposing screen. Antimicrob Agents Chemother 65:e01305-20. https://doi.org/10.1128/AAC.01305-20
50. Malo N, Hanley JA, Cerquozzi S, Pelletier J, Nadon R. 2006. Statistical practice in high-throughput screening data analysis. Nat Biotechnol 24:167–175. https://doi.org/10.1038/nbt1186
51. Brideau C, Gunter B, Pikounis B, Liaw A. 2003. Improved statistical methods for hit selection in high-throughput screening. J Biomol Screen 8:634–647. https://doi.org/10.1177/1087057103258285
52. Fuchs F, Hof H, Hofmann S, Kurzai O, Meis JF, Hamprecht A. 2021. Antifungal activity of nitroxoline against *Candida auris* isolates. Clin Microbiol Infect 27:1697. https://doi.org/10.1016/j.cmi.2021.06.035
53. de Oliveira HC, Castelli RF, Alves LR, Nosanchuk JD, Salama EA, Seleem M, Rodrigues ML. 2022. Identification of four compounds from the pharmakon library with antifungal activity against *Candida auris* and species of *Cryptococcus*. Med Mycol 60:myac033. https://doi.org/10.1093/mmy/myac033
54. Yousfi H, Ranque S, Cassagne C, Rolain JM, Bittar F. 2020. Identification of repositionable drugs with novel antimycotic activity by screening the prestwick chemical library against emerging invasive moulds. J Glob Antimicrob Resist 21:314–317. https://doi.org/10.1016/j.jgar.2020.01.002
55. Rybak JM, Muñoz JF, Barker KS, Parker JE, Esquivel BD, Berkow EL, Lockhart SR, Gade L, Palmer GE, White TC, Kelly SL, Cuomo CA, Rogers PD. 2020. Mutations in *Tac1B*: a novel genetic determinant of clinical fluconazole resistance in *Candida auris*. mBio 11:e00365-20. https://doi.org/10.1128/mBio.00365-20
56. Bing J, Hu T, Zheng Q, Muñoz JF, Cuomo CA, Huang G. 2020. Experimental evolution identifies adaptive aneuploidy as a mechanism of fluconazole resistance in *Candida auris*. Antimicrob Agents Chemother 65:e01466-20. https://doi.org/10.1128/AAC.01466-20
57. Carolus H, Pierson S, Muñoz JF, Subotić A, Cruz RB, Cuomo CA, Van Dijck P. 2021. Genome-wide analysis of experimentally evolved *Candida auris* reveals multiple novel mechanisms of multidrug resistance. mBio 12:e03333-20. https://doi.org/10.1128/mBio.03333-20
58. Li C, Wang J, Zhou B. 2010. The metal chelating and chaperoning effects of clioquinol: insights from yeast studies. J Alzheimers Dis 21:1249–1262. https://doi.org/10.3233/jad-2010-100024
59. Prasad R, Banerjee A, Khandelwal NK, Dhamgaye S. 2015. The Abcs of *Candida albicans* multidrug transporter Cdr1. Eukaryot Cell 14:1154–1164. https://doi.org/10.1128/EC.00137-15
60. Prasad R, Balzi E, Banerjee A, Khandelwal NK. 2019. All about CDR transporters: past, present, and future. Yeast 36:223–233. https://doi.org/10.1002/yea.3356
61. Znaidi S, Barker KS, Weber S, Alarco A-M, Liu TT, Boucher G, Rogers PD, Raymond M. 2009. Identification of the *Candida albicans* Cap1P regulon. Eukaryot Cell 8:806–820. https://doi.org/10.1128/EC.00002-09
62. Feng W, Yang J, Yang L, Li Q, Zhu X, Xi Z, Qiao Z, Cen W. 2018. Research of Mrr1, Cap1 and *MDR1* in *Candida albicans* resistant to azole medications. Exp Ther Med 15:1217–1224. https://doi.org/10.3892/etm.2017.5518
63. Sasse C, Schillig R, Reimund A, Merk J, Morschhäuser J. 2012. Inducible and constitutive activation of two polymorphic promoter alleles of the *Candida albicans* multidrug efflux pump *MDR1*. Antimicrob Agents Chemother 56:4490–4494. https://doi.org/10.1128/AAC.00264-12
64. Schubert S, Barker KS, Znaidi S, Schneider S, Dierolf F, Dunkel N, Aïd M, Boucher G, Rogers PD, Raymond M, Morschhäuser J. 2011. Regulation of efflux pump expression and drug resistance by the transcription factors Mrr1, Upc2, and Cap1 in *Candida albicans*. Antimicrob Agents Chemother 55:2212–2223. https://doi.org/10.1128/AAC.01343-10
65. Li J, Coste AT, Bachmann D, Sanglard D, Lamoth F. 2022. Deciphering the Mrr1/*MDR1* pathway in azole resistance of *Candida auris*. Antimicrob Agents Chemother 66:e0006722. https://doi.org/10.1128/aac.00067-22
66. Biermann AR, Hogan DA. 2022. Transcriptional response of *Candida auris* to the Mrr1 inducers methylglyoxal and benomyl. mSphere 7:e0012422. https://doi.org/10.1128/msphere.00124-22
67. Shukla S, Sauna ZE, Prasad R, Ambudkar SV. 2004. Disulfiram is a potent modulator of multidrug transporter Cdr1P of *Candida albicans*. Biochem Biophys Res Commun 322:520–525. https://doi.org/10.1016/j.bbrc.2004.07.151
68. Xu Y, Lu H, Zhu S, Li W-Q, Jiang Y-Y, Berman J, Yang F. 2021. Multifactorial mechanisms of tolerance to ketoconazole in *Candida albicans*. Microbiol Spectr 9:e0032121. https://doi.org/10.1128/Spectrum.00321-21
69. Wasi M, Khandelwal NK, Moorhouse AJ, Nair R, Vishwakarma P, Bravo Ruiz G, Ross ZK, Lorenz A, Rudramurthy SM, Chakrabarti A, Lynn AM, Mondal AK, Gow NAR, Prasad R. 2019. ABC transporter genes show upregulated expression in drug-resistant clinical isolates of *Candida auris*: a genome-wide characterization of ATP-binding cassette (ABC) transporter genes. Front Microbiol 10:1445. https://doi.org/10.3389/fmicb.2019.01445
70. Zhang H, Niu Y, Tan J, Liu W, Sun MA, Yang E, Wang Q, Li R, Wang Y, Liu W. 2019. Global screening of genomic and transcriptomic factors associated with phenotype differences between multidrug-resistant and -susceptible *Candida haemulonii* strains. mSystems 4:e00459-19. https://doi.org/10.1128/mSystems.00459-19
71. Saini P, Gaur NA, Prasad R. 2006. Chimeras of the ABC drug transporter Cdr1P reveal functional indispensability of transmembrane domains and nucleotide-binding domains, but transmembrane segment 12 is replaceable with the corresponding homologous region of the non-drug transporter Cdr3P. Microbiology (Reading) 152:1559–1573. https://doi.org/10.1099/mic.0.28471-0
72. Gershon H, McNeil MW, Parmegiani R, Godfrey PK. 1972. Antifungal activity of 7- and 5,7-substituted 8-quinolinols. J Med Chem 15:987–989. https://doi.org/10.1021/jm00279a028
73. Gershon H, Parmegiani R, Godfrey PK. 1972. Antifungal activity of 5-, 7-, and 5,7-substituted 2-methyl-8-quinolinols. Antimicrob Agents Chemother 1:373–375. https://doi.org/10.1128/AAC.1.5.373
74. Gershon H, McNeil MW, Parmegiani R, Godfrey PK. 1972. Secondary mechanisms of antifungal action of substituted 8-quinolinols. 3. 5,7,8-substituted quinolines. J Med Chem 15:105–106. https://doi.org/10.1021/jm00271a033
75. Treiber C, Simons A, Strauss M, Hafner M, Cappai R, Bayer TA, Multhaup G. 2004. Clioquinol mediates copper uptake and counteracts copper efflux activities of the amyloid precursor protein of Alzheimer's disease. J Biol Chem 279:51958–51964. https://doi.org/10.1074/jbc.M407410200
76. Tardiff DF, Brown LE, Yan X, Trilles R, Jui NT, Barrasa MI, Caldwell KA, Caldwell GA, Schaus SE, Lindquist S. 2017. Dihydropyrimidine-thiones and clioquinol synergize to target B-amyloid cellular pathologies through a metal-dependent mechanism. ACS Chem Neurosci 8:2039–2055. https://doi.org/10.1021/acschemneuro.7b00187
77. Yan C, Wang S, Wang J, Li H, Huang Z, Sun J, Peng M, Liu W, Shi P. 2018. Clioquinol induces G_2/M cell cycle arrest through the up-regulation of TDH3 in *Saccharomyces Cerevisiae*. Microbiol Res 214:1–7. https://doi.org/10.1016/j.micres.2018.05.006
78. You Z, Zhang C, Ran Y. 2020. The effects of clioquinol in morphogenesis, cell membrane and ion homeostasis in *Candida albicans*. BMC Microbiol 20:165. https://doi.org/10.1186/s12866-020-01850-3
79. Montoya MC, Beattie S, Alden KM, Krysan DJ. 2020. Derivatives of the antimalarial drug mefloquine are broad-spectrum antifungal molecules with activity against drug-resistant clinical isolates. Antimicrob Agents Chemother 64:e02331-19. https://doi.org/10.1128/AAC.02331-19

80. Mao X, Schimmer AD. 2008. The toxicology of clioquinol. Toxicol Lett 182:1–6. https://doi.org/10.1016/j.toxlet.2008.08.015
81. Perez DR, Sklar LA, Chigaev A. 2019. Clioquinol: to harm or heal. Pharmacol Ther 199:155–163. https://doi.org/10.1016/j.pharmthera.2019.03.009
82. Nakae K, Yamamoto S, Shigematsu I, Kono R. 1973. Relation between subacute myelo-optic neuropathy (S.M.O.N.) and clioquinol: nationwide survey. Lancet 1:171–173. https://doi.org/10.1016/s0140--6736(73)90004-4
83. Tsubaki T, Honma Y, Hoshi M. 1971. Neurological syndrome associated with clioquinol. Lancet 1:696–697. https://doi.org/10.1016/s0140-6736(71)92699-7
84. Asao M. 1979. Clioquinol and S.M.O.N.: Reanalysis of original data. Lancet 1:446. https://doi.org/10.1016/s0140-6736(79)90928-0
85. Meade TW. 1975. Subacute myelo-optic neuropathy and clioquinol. An epidemiological case-history for diagnosis. Br J Prev Soc Med 29:157–169. https://doi.org/10.1136/jech.29.3.157
86. Matlack KES, Tardiff DF, Narayan P, Hamamichi S, Caldwell KA, Caldwell GA, Lindquist S. 2014. Clioquinol promotes the degradation of metal-dependent amyloid-B (Aβ) oligomers to restore endocytosis and ameliorate Aβ toxicity. Proc Natl Acad Sci U S A 111:4013–4018. https://doi.org/10.1073/pnas.1402228111
87. Ding W-Q, Liu B, Vaught JL, Yamauchi H, Lind SE. 2005. Anticancer activity of the antibiotic clioquinol. Cancer Res 65:3389–3395. https://doi.org/10.1158/0008-5472.CAN-04-3577
88. Daniel KG, Chen D, Orlu S, Cui QC, Miller FR, Dou QP. 2005. Clioquinol and pyrrolidine dithiocarbamate complex with copper to form proteasome inhibitors and apoptosis Inducers in human breast cancer cells. Breast Cancer Res 7:R897–908. https://doi.org/10.1186/bcr1322
89. Chen D, Cui QC, Yang H, Barrea RA, Sarkar FH, Sheng S, Yan B, Reddy GPV, Dou QP. 2007. Clioquinol, a therapeutic agent for Alzheimer's disease, has proteasome-inhibitory, androgen receptor-suppressing, apoptosis-inducing, and antitumor activities in human prostate cancer cells and xenografts. Cancer Res 67:1636–1644. https://doi.org/10.1158/0008-5472.CAN-06-3546
90. Ritchie CW, Bush AI, Mackinnon A, Macfarlane S, Mastwyk M, MacGregor L, Kiers L, Cherny R, Li QX, Tammer A, Carrington D, Mavros C, Volitakis I, Xilinas M, Ames D, Davis S, Beyreuther K, Tanzi RE, Masters CL. 2003. Metal-protein attenuation with iodochlorhydroxyquin (clioquinol) targeting Abeta amyloid deposition and toxicity in Alzheimer disease: a pilot phase 2 clinical trial. Arch Neurol 60:1685–1691. https://doi.org/10.1001/archneur.60.12.1685
91. Lund EK, Wharf SG, Fairweather-Tait SJ, Johnson IT. 1998. Increases in the concentrations of available iron in response to dietary iron supplementation are associated with changes in crypt cell proliferation in rat large intestine. J Nutr 128:175–179. https://doi.org/10.1093/jn/128.2.175
92. Spottiswoode N, Pet D, Kim A, Gruenberg K, Shah M, Ramachandran A, Laurie MT, Zia M, Fouassier C, Boutros CL, Lu R, Zhang Y, Servellita V, Bollen A, Chiu CY, Wilson MR, Valdivia L, DeRisi JL. 2023. Successful treatment of *Balamuthia mandrillaris* granulomatous amebic encephalitis with nitroxoline. Emerg Infect Dis 29:197–201. https://doi.org/10.3201/eid2901.221531
93. Woodworth MH, Dynerman D, Crawford ED, Doernberg SB, Ramirez-Avila L, Serpa PH, Nichols A, Li LM, Lyden A, Tato CM, Miller S, Derisi JL, Langelier C. 2019. Sentinel case of *Candida auris* in the Western United States following prolonged occult colonization in a returned traveler from India. Microb Drug Resist 25:677–680. https://doi.org/10.1089/mdr.2018.0408
94. Odds FC, Brown AJP, Gow NAR. 2004. *Candida albicans* genome sequence: a platform for genomics in the absence of genetics. Genome Biol 5:230. https://doi.org/10.1186/gb-2004-5-7-230
95. Aszalos A, Robison RS, Lemanski P, Berk B. 1968. Trienine, an antitumor triene antibiotic. J. Antibiot 21:611–615. https://doi.org/10.7164/antibiotics.21.611
96. Maestrone G, Semar R. 1968. Establishment and treatment of cutaneous *Candida albicans* infection in the rabbit. Naturwissenschaften 55:87–88. https://doi.org/10.1007/BF00599501
97. Meyers E, Miraglia GJ, Smith DA, Basch HI, Pansy FE, Trejo WH, Donovick R. 1968. Biological characterization of prasinomycin, a phosphorus-containing antibiotic. Appl Microbiol 16:603–608. https://doi.org/10.1128/am.16.4.603-608.1968
98. Sullivan DJ, Westerneng TJ, Haynes KA, Bennett DE, Coleman DC. 1995. *Candida dubliniensis* SP. Nov.: phenotypic and molecular characterization of a novel species associated with oral candidosis in HIV-infected individuals. Microbiology (Reading) 141 (Pt 7):1507–1521. https://doi.org/10.1099/13500872-141-7-1507
99. Ennis CL, Hernday AD, Nobile CJ. 2021. A Markerless CRISPR-mediated system for genome editing in *Candida auris* reveals a conserved role for Cas5 in the caspofungin response. Microbiol Spectr 9:e0182021. https://doi.org/10.1128/Spectrum.01820-21
100. Nguyen N, Quail MMF, Hernday AD. 2017. An efficient, rapid, and recyclable system for CRISPR-mediated genome editing in *Candida albicans*. mSphere 2:e00149-17. https://doi.org/10.1128/mSphereDirect.00149-17
101. Seher TD, Nguyen N, Ramos D, Bapat P, Nobile CJ, Sindi SS, Hernday AD, Andrews BJ. 2021. Addtag, a two-step approach with supporting software package that facilitates CRISPR/CAS-mediated precision genome editing. G3 Genes|Genomes|Genetics 11. https://doi.org/10.1093/g3journal/jkab216
102. Horst JA, Wu W, DeRisi JL. 2017. Minorityreport, software for generalized analysis of causal genetic variants. Malar J 16:90. https://doi.org/10.1186/s12936-017-1730-2
103. Danecek P, Bonfield JK, Liddle J, Marshall J, Ohan V, Pollard MO, Whitwham A, Keane T, McCarthy SA, Davies RM, Li H. 2021. Twelve years of Samtools and BCFtools. Gigascience 10:giab008. https://doi.org/10.1093/gigascience/giab008
104. Team RC. 2019. R: a language and environment for statistical computing. R Foundation for Statistical Computing. https://www.R-project.org
105. Wickham H, Averick M, Bryan J, Chang W, McGowan L, François R, Grolemund G, Hayes A, Henry L, Hester J, Kuhn M, Pedersen T, Miller E, Bache S, Müller K, Ooms J, Robinson D, Seidel D, Spinu V, Takahashi K, Vaughan D, Wilke C, Woo K, Yutani H. 2019. Welcome to the Tidyverse. JOSS 4:1686. https://doi.org/10.21105/joss.01686